Boulder Atmosphere Innovation Research

Boulder A.I.R. L.L.C; 2820 Lafayette Dr., Boulder, CO 80305, U.S.A.; dh.bouldair@gmail.com

January 13, 2021

To:

City of Longmont
350 Kimbark Street
Longmont, CO 80501

Attn: Dr. Jane Turner

Re: Longmont Regional Air Quality Study – Year 2020 Quarter 2 Report

Dear Dr. Turner,

Please find included with this letter the revised April – June (Quarter 2) 2020 report for our work on the Longmont Air Quality Study. The monitoring data and data interpretations are presented.

Thank you for providing this opportunity to provide air quality monitoring to the City of Longmont and its citizens. We would be happy to discuss any questions that you, other City staff or Longmont citizens may have.

Sincerely,

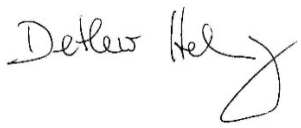

Detlev Helmig

Boulder AIR LLC

2020 Quarter 2 (April – June) Report

Longmont Air Quality Study

Executive Summary

This report summarizes the data and preliminary findings from the Longmont Air Quality Study during April through June of 2020. This was the first quarter when both the Longmont Municipal Airport (LMA) and the Longmont Union Reservoir (LUR) monitoring sites were fully operational and reporting data for the full quarter. All variables were reported in near-real time on the public *Longmont Air Quality Now* web portal.

This report includes graphical analyses of all data acquired during the 2nd quarter (Q2). In addition, data comparisons and analyses of selected events that resulted in elevated concentrations are presented. LMA and LUR data are compared with each other and also with concurrent observations from the Boulder Reservoir.

The ozone National Ambient Air Quality Standard (NAAQS) was exceeded a total of five times in Q2 at the two sites (four times at LMA, and one time at LUR). A remarkable finding was a dramatic reduction in the number of episodes when elevated levels of volatile organic compounds (VOCs) were observed after early April. For example, during the month of March, there were almost daily occurrences of ethane reaching 100-500 ppb and benzene reaching 2-8 ppb. However, starting in mid-April and continuing through the rest of the 2nd quarter, ethane never exceeded 100 ppb, and there was only one occasion when benzene was above 1 ppb. In this report, we also present a number of correlation analyses where we explore the ratios and behavior of selected VOCs from measurements taken at LUR as a function of their source sector using wind speed and direction correlation analyses. These studies revealed a number of distinct differences in the VOC signatures, showing a clear influence from oil and gas emissions transported from the north to southeast sectors, versus urban source signatures from air that is brought in from the west (the City of Longmont). Much in contrast to VOCs, nitrogen oxides at LUR appear to have a stronger urban source originating from the City of Longmont than from sectors containing oil and gas activities.

An unexpected and unprecedented event during Q2 was the reduction in traffic and certain industrial activities due to restrictions that were implemented in mid-March to slow down the spread of the COVID-19 virus. There has been great interest in if and to what degree these restrictions may have impacted atmospheric emissions and air quality. Comparison data from either prior or later years during the same seasonal time window are required for investigating this question. Unfortunately, the Longmont monitoring data record is too short to draw any conclusions at this time.

Table of Contents

1. Project Scope and Goals

No changes from Q1 report.

2. Overview of the Monitoring Program

No changes from Q1 report.

3. Air Quality Monitoring Study Updates

No changes from Q1 report.

4. Data Quality Assurance/Quality Control Process

No Changes from Q1 report.

5. Website Development

The webcam at LMA was lost on June 17 due to a landscaping accident and there were no webcam pictures reported for this site for the remainder of quarter 2. There are no other changes to report since Q1.

6. Data Archiving

No Changes from Q1 report.

7. Data for Quarter 2, 2020

There were two episodes with brief interruption of the monitoring. In both instances, these resulted from facility problems:

On April 4, there was a failure of the LUR building air handling system that resulted in an overheating of the inside where the temperature reached 145°F. The cause of this failure was a stuck air diverting flap that prevented colder air from reaching the interior. The air handling system was repaired on April 8. The monitors were turned back on and resumed operation on the same day.

This overheating event put the analytical instrumentation at high risk for damage and failure as the electronics are not configured to tolerate such high temperatures. All systems were manually shut off as soon as the overheating was noticed. We have now also implemented automated temperature check routines. A script was developed that checks the room temperature every minute. When the temperature exceeds a threshold value set to 86°F, an e-mail alert is sent to Boulder AIR personnel. In order to minimize future down time and protect the instrumentation, all major equipment items are

now powered through an 8-circuit netswitch that has an external temperature probe. Each outlet is automatically switched off when a temperature above a pre-set value is exceeded.

The second event occurred on June 17 at LMA when a landscaping contractor accidentally hit one of the tower guy wires with a riding lawn mower. This caused the upper section of the tower to collapse. The damage resulted in eight days of lost wind measurements. To continue sampling, the gas inlets were attached to the remaining bottom tower segment, which resulted in a temporary lower sampling height (3 m instead of 8 m). Further, the cable to the webcam was severed, which resulted in the loss of the recording of webcam pictures. The tower was repaired on June 24 and all measurements (except the webcam) resumed normal operation the same day.

The data that were recorded in Q2, 2020, are included in this report in graphical time series format in Supplement A (LMA) and Supplement B (LUR). These graphs provide the records of the completeness of the data coverage and general features in the dynamic, diurnal, and seasonal changes. Some of the data (e.g. wind direction) are difficult to interpret when 3 months of data are included in the same plot. In these instances, the primary objective is to show general trends and that the data are nearly continuous – not to point out individual features. Data coverage for all variables is >95% for the full quarter.

In Supplement C, the variables that are measured at both sites are shown together in a set of time series graphs. These graphs are presented to highlight similarities and differences between the two locations.

8. Selected Data Examples and Preliminary Interpretations

COVID-19

An unexpected and unprecedented event during Q2 was the reduction in traffic and certain industrial activities due to restrictions that were implemented in mid-March to slow down the spread of the COVID-19 virus. Traffic dropped to a trickle during Colorado's month-long stay-at-home order from March 27 through April 27, and only slowly resumed to near-normal levels in late May. There has been great interest in if and to what degree these restrictions may have impacted atmospheric emissions and air quality. Unfortunately, the Longmont monitoring data are too short at this time to draw any conclusions about this question. Atmospheric concentrations depend on a myriad of influences. Among these, seasonal changes in meteorology, and the year-to-year variability of weather conditions are very strong forces, which influence conditions dramatically. Particularly during spring, atmospheric concentrations that result from nearby pollution sources drop strongly because of the increase in solar radiation, which (1) shortens and weakens nighttime inversions that can trap pollution near the surface, and (2) deeper boundary layer depths and stronger vertical mixing from turbulent transport caused by the surface heating. Since COVID-19's impacts happened during spring, it is therefore not possible to deduce if and how much of the concentration declines during spring were caused by these natural effects versus reduced emissions. The investigation of the COVID lockdown requires comparison data from prior or later years collected at the same location and during the same seasonal time window. Since 2020 was the first year of springtime measurements at LMA and LUR, those comparison data are unfortunately not available. This analysis has been attempted for the Boulder Reservoir data, where four years of data are available. These studies show a probable reduction in nitrogen oxides levels, on the order of 25% compared to the three prior years. There were no notable reductions for other pollutants, i.e. VOCs (ethane, propane, benzene) and ozone (presentation by D. Helmig to Boulder County commissioners, Oct. 8, 2020).

Ozone

The full Q2 ozone records for LMA and LUR are presented in Figures SA8 and SB8. In comparison to Q1, ozone displays a more dynamic behavior, with a wider spread between the lowest and highest values, spanning a range of < 1 ppb to 89 ppb. This reflects that during the late spring and early summer months, atmospheric ozone levels began increasing towards their seasonal peak, which typically occurs during the late summer months of July and August in Colorado. Figures SA9 and SB9 show the ozone data averaged to a moving 8-hour average, which is the metric used for the National Ambient Air Quality Standard (NAAQS). Four exceedances of the NAAQS were observed during Q2 at LMA, and one exceedance was recorded at LUR. The first ozone exceedance of the year that was observed on April 17 is remarkably early in the season, as in the Colorado Front Range ozone values above 70 ppb are usually not observed until about one month later. This ozone event occurred during conditions with snow cover and a shallow, stable boundary layer, which allowed ozone precursor pollutants to build up to elevated levels near the surface. The high solar irradiance, enhanced by reflected light from the snow surface, was another contributing factor for the ozone buildup. During this period, ozone was highest at the sites nearest to the mountain slopes (LMA and the Boulder Reservoir (BRZ)). At LUR and in Broomfield (which are farther east), the 8-hour mean ozone remained below the 70 ppb NAAQS limit. The highest 8-hour ozone exceedance during Q2 was recorded on June 17 at LUR with 75.6 ppb.

Figure 1 shows a summary of the ozone data that compares the median and variability from the two Longmont sites to the observations from BRZ and the Broomfield Soaring Eagle Park (BSE) sites. This analysis illustrates the gradual increase in ozone heading into the summer months. Figure 1 also shows that on average surface ozone levels in Longmont are lower than at the comparison sites, which is a trend consistent with levels seen during Q1.

CO_2

The full Q2 CO_2 records are available in Figures SA6 and SB6 for LMA and LUR, respectively. Mole fractions of CO_2 exhibited an opposite trend to ozone and decreased marginally during Q2 when compared with Q1 CO_2 levels. This is most likely due to two effects: 1. During summer, the lower atmosphere mixes more vigorously due to convection, driven by more available sunlight. This increased mixing promotes stronger dilution of the CO_2-enriched surface air with the cleaner, lower CO_2-air from aloft. 2. Photosynthesis by the biosphere is much stronger during the summer. This drives an uptake/removal of CO_2 from the atmosphere. Figure 2 shows the median CO_2 values illustrated by the black line in the middle of each colored box decreased to around 420 ppm by June. Q1 median CO_2 values at LMA and LUR were 425-430 ppm. The wind dependency analyses in Figure 3 illustrate that the dominant CO_2 contributions are from the west at low wind speeds. Since the LUR site is east of the city, this suggests that the city is the primary source for enhanced CO_2 observed at LUR. However, a specific source for the high CO_2 mole fractions seen in winds from the west of LMA is unclear and is under investigation.

Methane

The full Q2 methane records are available in Figures SA7 and SB7 for LMA and LUR, respectively. Similar to CO_2, methane mole fractions trended downward during Q2 (Figure 4). This also shows that both LMA and LUR recorded more variability and larger values at the higher percentile margins than at sites in neighboring cities. Among the two Longmont sites, LUR has higher absolute values and variance when compared with LMA. This is likely due to its proximity to oil and gas operations northeast of the City.

This interpretation is supported by the wind dependency analyses in Figures 5-7. Figure 5 shows a selected example, with a large methane spike at LUR, when winds were from the north and north east. That peak quickly dissipated as soon as the winds shifted to the southwest. This suggests a strong methane source northeast of the City. Figure 6 shows that this particular methane event was also associated with an increase in CO_2. Just prior to the June 29, event, at ~9:00 pm, the wind speed was low (< 2 m s^{-1}) from the NE. Low wind speeds in combination with the development of the nocturnal boundary layer and a source region to the northeast allowed the methane concentrations to build up to over six times background levels. Similar increases in NO_x and CO_2 were observed at the same time. Figure 7 shows the dependency of methane concentrations with wind speed and direction for the entire quarter. Analysis of individual transport events has yielded the consistent finding that transport from the northeast sector on average brings significantly higher methane concentrations to LUR and LMA than from other wind directions. Several other similar short-lived methane peaks were reported at LUR during Q1.

VOCs

The full Q2 LUR records for six selected VOCs are available in Figures SB10–SB16. Mole fractions of many oil and gas associated VOCs decreased remarkably during Q2 when compared with Q1, with a notable decrease from late March to early April. In the following section, data analyses are presented that support the conclusion that these decreases most likely stem from reduced remission rates at well sites nearby the LUR monitoring site.

Figure 8 shows a series of graphs for an illustration of this decrease in VOC levels. The time series data for ethane and benzene from LUR and BRZ are overlaid in panels (a) and (b) of Figure 8. These emission changes were further investigated using the natural gas emissions tracer ethane. Panels (c) and (d) shows the LUR and BRZ ethane results as individual time series to better illustrate the relative changes from February to May. During February-March, the LUR VOCs data show a much larger abundance of high concentration peaks. After mid-April, VOC concentrations at the two sites became more similar. It is noteworthy that these concentration drops occurred shortly after the posting of the LUR VOCs results to the *Longmont Air Quality Now* website (March 20th) and the publishing of several newspaper reports of these recordings (Boulder Daily Camera April 13, 27, and Longmont Times Call April 13, 25). This timely decrease suggests that publishing our findings may have brought added attention to these emissions, which then could have led to efforts to mitigate the emissions. This hypothesis is supported by a series of further analyses: Ethane data for February - May for each month were analyzed for their statistical distribution (e). The monthly 5, 25, 50, 75, and 95 percentile values were then normalized to the February values and plotted against the month (f). The curves deviate progressively more towards the high percentile values. For the 95th percentile values, BRZ ethane values drop to ~40% of their February maximum by the month of May. For LUR, the corresponding value is ~10%, which is a difference of approximately a factor of 4 between both sites. The same comparison of the 75th percentile results yields approximately a factor of 3 difference. For the medians it's about a factor of 2. If the emission drops would have been a large geographical scale effect, impacting the air composition of the entire region as a whole, then similar rates of decline would be expected for both sites. The stark difference in these decline rates, particularly being more pronounced at the high percentile values (reflecting the occurrence of short, extremely high concentration spikes), is an indication that emissions reductions in the near vicinity of the LUR monitoring site, most likely within a few miles, were much more significant than for the wider Front Range Region as a whole.

The statistical analysis of three further VOCs in Figure 9 exemplifies the conclusion from the ethane analysis and the differences between quarters 1 and 2. The median values for all plotted VOCs were significantly lower in Q2 compared to Q1. In addition, the variability (as seen by the height of the boxes and whiskers) was much lower in Q2. Again, this indicates that the largest change was seen in the reduction of the peak values. Figure 10 compares the distribution of three VOCs between LUR and BRZ during April - June. While LUR data are higher for all compounds during all three Q2 months, the relative difference became progressively smaller throughout this three-month comparison, with the LUR benzene values even dropping below BRZ readings during the latter part of Q2.

Figure 11 provides an investigation of potential changes in the footprint of upwind emissions sources. There is no striking difference between the two quarters for the light alkanes, which are primary oil and gas emissions. This suggests that the contributing VOC source areas remained constant, albeit with reduced emission strength. A somewhat different behavior is seen for benzene, where transport from the western sector became more important, which is likely due to transport from the north becoming weaker/less significant. Nonetheless, eight of the ten highest benzene peaks were transported from northern sectors, as can be seen in Figure 12.

In conclusion, these analyses show that emissions reductions in the near vicinity of the LUR monitoring site, most likely within a few miles, were more significant than for the wider Front Range Region as a whole. As hypothesized above, this might be explained by the publishing of the monitoring results, which may have helped bring attention to and to reducing these emissions. There is also the possibility that production activities and associated emissions due to the crash of the oil market in spring 2020, at well sites near LUR (i.e. within a few miles), may have possibly been reduced to a significantly larger degree than across the Denver Julesburg Basin as a whole. This also could potentially have caused the disproportional reduction in observed concentrations at LUR compared to BRZ. However, if this was the case, then one would expect a return to the large difference in the data seen earlier in the year as the oil market recovered during the latter part of the year. The Q3 and Q4 data do not show this behavior and therefore do no support this hypothesis (to be shown in the upcoming reports). A further investigation of this question could possibly be pursued by a comparison of production rates from well sites near LUR with those from the DJB as a whole.

Relationships between VOC pairs are investigated in Figure 13. The upper graphs use propane, a natural gas tracer, as the reference VOC. The figure also includes comparisons of the pentane isomers, and the benzene/toluene ratio. While there is a clear correlation between individual VOC species (as shown in Figure 13 panels), these ratios are also influenced by wind speed and direction. Transport from the northeast sector brings in air that is relatively rich in propane and benzene. The low i/n-pentane ratio of ~0.9 is indicative of a dominant influence by primary oil and gas emissions (Figure 13). The higher i/n-pentane ratios of 1.4-1.5 from the south and west sectors are more influenced by background and urban emissions. Both the propane/ethane, and the benzene/toluene ratios show maximum values for the 20-30 degrees sector (northeast), which identifies that sector as the one with the most significant influence from with oil and natural gas activities.

Nitrogen Oxides (NO, NOx)

The Q2 LUR records for NO and NO_x are shown in Figures SB17 and SB18, respectively. Please note that these NO_x data are preliminary and are currently undergoing further quality control. The original NO_x analyzer was a Thermo Scientific 42iQ instrument. It was replaced with a newly purchased Teledyne T200UP analyzer on June 24. While we maintained the same calibration standard and protocol, these two instruments differ in the technique for determining NO_2. The basic measurement in both

instruments is made by producing ozone inside the instrument and reacting this with NO from the sample. The rapid reaction of NO + O_3 produces NO_2 and light. The light intensity is directly proportional the amount of NO and is used to calculate the ambient NO concentration. To measure NO_x, the NO_2 in the air sample is converted to NO. This measurement includes the original NO from the sample plus the NO that was converted from NO_2, with the sum being measured as NO_x. To convert NO_2 to NO, a heated molybdenum oxide catalyst is used in the Thermo Scientific instrument, and a photolytic converter is used in the Teledyne instrument. Both instruments specify a conversion efficiency of greater than 95%. However, it is possible that the Thermo Scientific monitor detects other oxidized nitrogen species in ambient air (such as HNO_2, HNO_3 or N_2O_5), as those may be converted similarly to NO by the heated catalyst. Both instruments were co-located at LUR and sampled the same air from June 12-16. Results and interpretation from this experiment will be presented in the Q3 report. Higher NO_x levels were observed at LUR compared to the other network locations for all months. The wind analysis in Figure 16 shows that the highest concentrations are observed when transport is from the northwest to southwest sectors, which is the direction of the City of Longmont. This demonstrates a different source region than what was observed for the VOCs discussed above. The data show two spikes when NO exceeded 300 ppb. During these spikes, NO_2 was low since the NO and NO_x values are approximately equal. Both of these events occurred during the daytime (around noon and at 5 p.m.). During the day, in the presence of ozone, NO will quickly (within a few minutes) convert to NO_2. Therefore, these two spikes most likely originated from a source very near to the recording station. We suspect that these spikes occurred from vehicle emissions at the nearby turnaround of the access road or possibly from tractors being operated on the nearby farmland to the west.

Particulate Matter (PM)

The time series plots for PM10 and PM2.5 at LUR during Q2 presented in Figures SB19 and SB20. Box whisker plots that summarize the monthly PM2.5 and PM10 concentrations for LUR and BSE are shown in Figure 17. PM2.5 concentrations from LUR and BSE were similar with monthly median values between 3 and 5 $\mu g\ m^{-3}$. These statistical analyses confirm our previous conclusion (stated in Q1 report) that PM pollutant levels are relatively homogeneous on a larger geographical scale, except when influenced by unusual events such as wildfires. The NAAQS for PM2.5 and PM10 are 35 $\mu g\ m^{-3}$ and 150 $\mu g\ m^{-3}$, respectively, over a 24 hour period. Figures SB18 and SB19 show brief periods with elevated particulate concentrations. These are typically short-lived episodes (several minutes to 1 hour). But as can be seen in Figure 17, average PM concentrations at LUR and BSE were significantly below these limits for all of Q2.

Figures

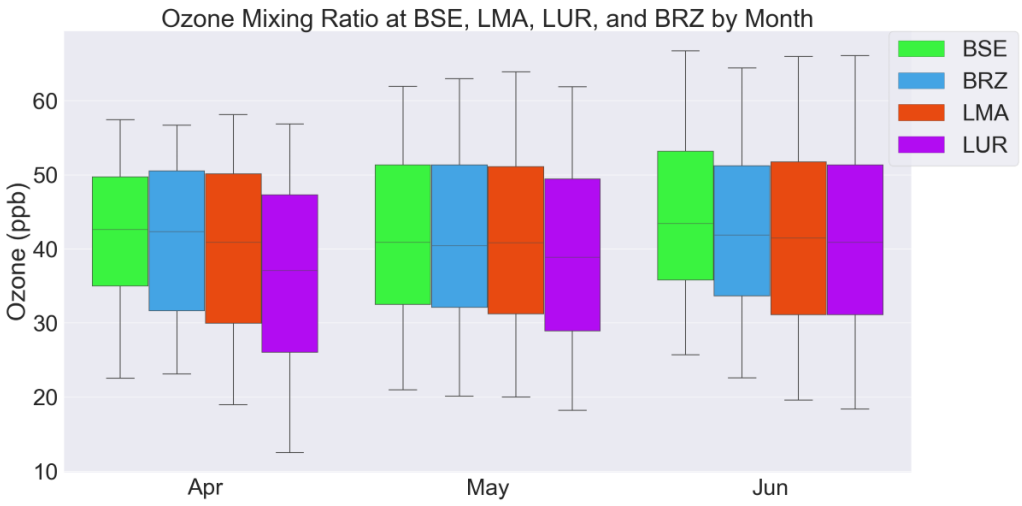

Figure 1:
Comparison of the ozone distribution at the Broomfield Soaring Eagle (BSE), Boulder Reservoir (BRZ), LMA, and LUR during April – June 2020. These box whisker plots show the median value as the center line, the 25-75 percentile distribution as the colored boxes, and the 5-percentile and 95-percentile values as the whiskers. The two Longmont sites show a relatively higher variability, indicative of a more dynamic ozone chemistry. The graphs also show the increase in the higher percentile values towards the summer ozone season.

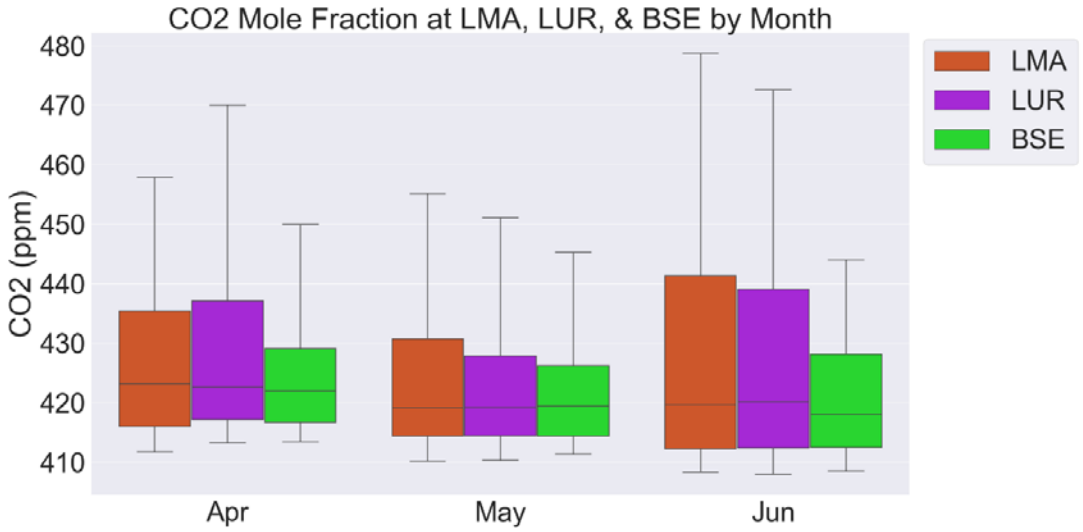

Figure 2:
Comparison of the CO_2 distribution at LMA, LUR, and BSE during April – June 2020. The features of the box and whisker limits are the same as described in Figure 1. A striking feature are the higher high percentile values, indicating more or stronger CO_2 sources in the vicinity of the Longmont sites (compared to Broomfield).

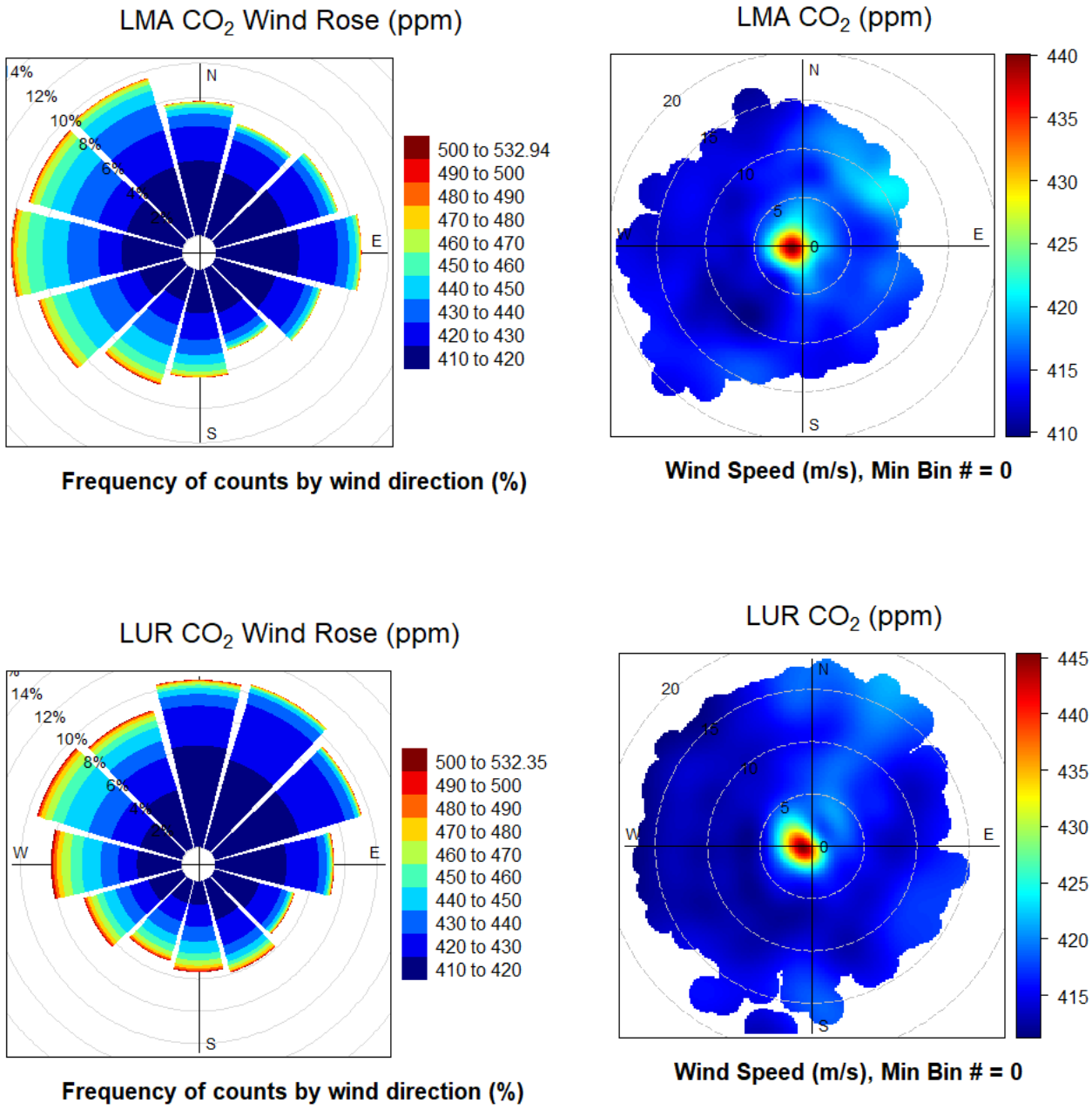

Figure 3:
Wind rose (left) and wind heat map analysis showing the dependency of CO_2 mole fractions at LMA (top) and LUR (bottom) during April – June 2020. For both sites, the strongest CO_2 sources appear to be to the west of the monitoring site location. The Min Bin number is a filter that is used on occasion to reject data bins that have a low number of data. In this case, with Min Bin # = 0, no bins were rejected.

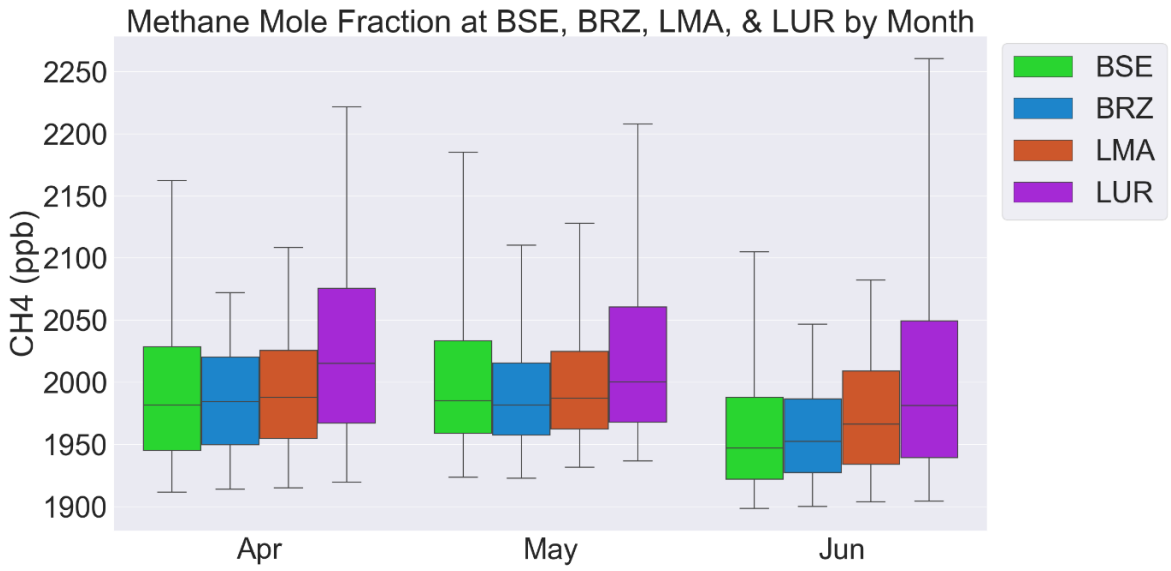

Figure 4:
Comparison of the methane distribution at BSE, BRZ, LMA, and LUR during April – June 2020. LUR shows consistently the highest methane (at all percentiles) among these four sites. See Figure 1 for explanation of the box and whisker plot formats.

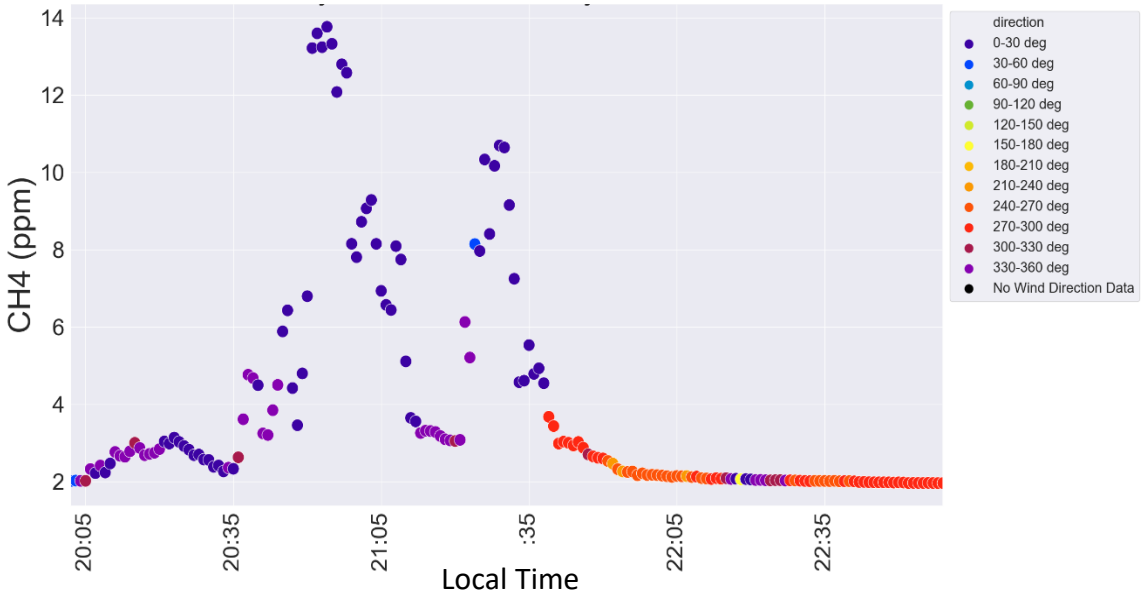

Figure 5:
Time series of the largest methane peak observed at LUR during Q2 on June 29. The x-axis lists an approximate 3-hour time interval starting before and ending after the peak event. Data points are color coded by wind direction. The wind direction in the one hour before the concentration peak was from the northeast with a wind speed of 1-2 m/s. it took some time for the plume to arrive at LUR. During the time the plume was moving through, the wind was from the north, but that may not be the original source region.

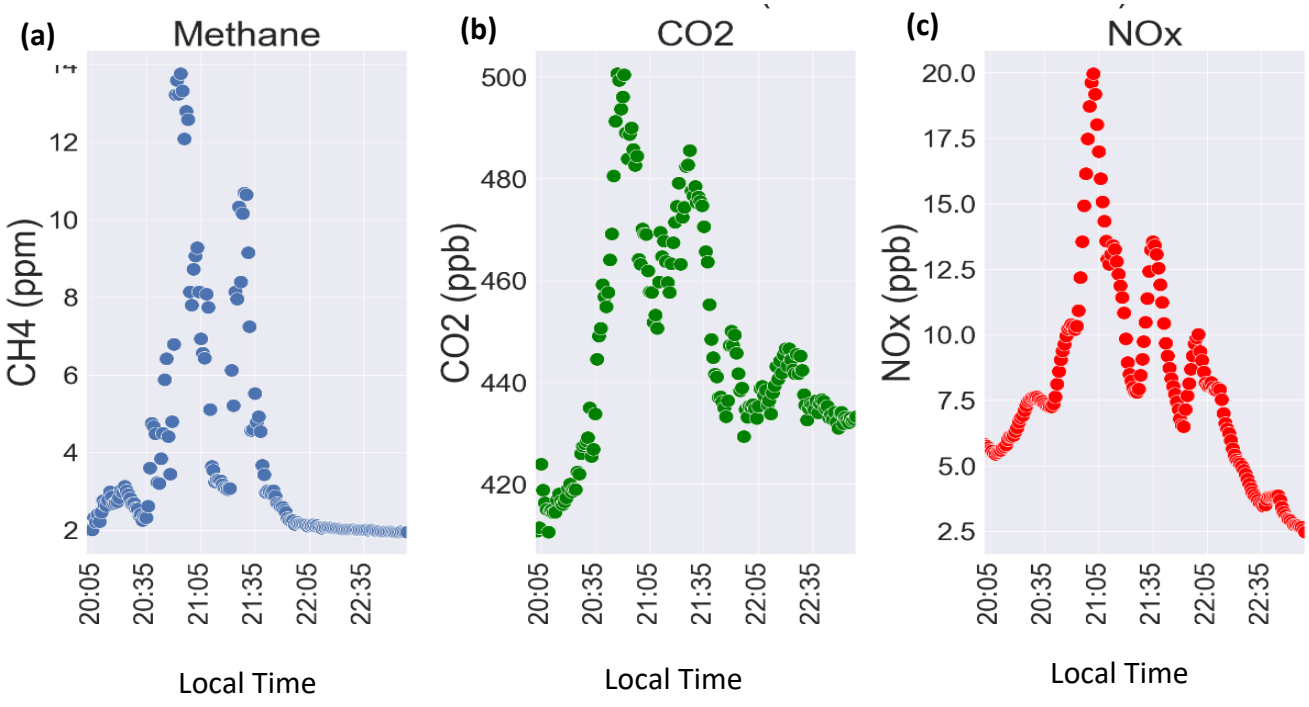

Figure 6:
Same peak as in Figure 5 plotted with CO_2 (b), and NO_x (c). The methane spike coincided with increases in CO_2 and NO_x. However, the timing was slightly offset, suggesting that several different sources within the same wind sector may have contributed to these concentration increases.

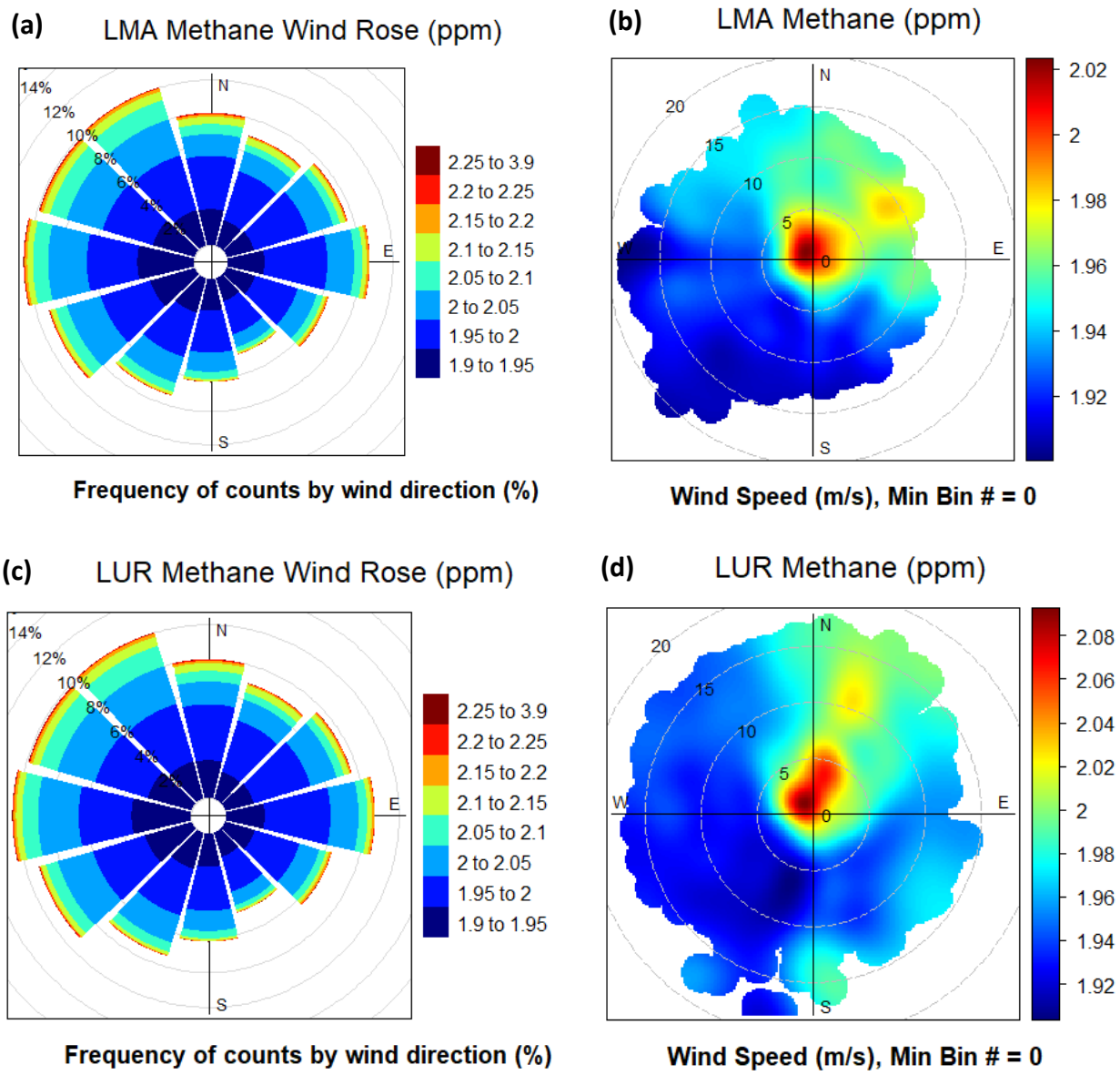

Figure 7:
Concentration wind rose (left) and wind heat map analysis (right) showing the dependency of methane mole fractions at LMA (top) and LUR (bottom) during April – June 2020. Both sites see transport of elevated methane predominantly during winds from the northeast sector. The Min Bin number is a filter that is used on occasion to reject data bins that have a low number of data. In this case, with Min Bin # = 0, no bins were rejected.

Figure 8:
Ethane (a) and benzene (b) time series graphs comparing the recordings at LUR and BRZ from February 1st – Jun 30th overlaid in one graph. LUR shows a much higher frequency of concentration spikes, and resulting higher concentrations, during the earlier part of the plotted time interval. The behavior was more alike after approximately mdi-April.

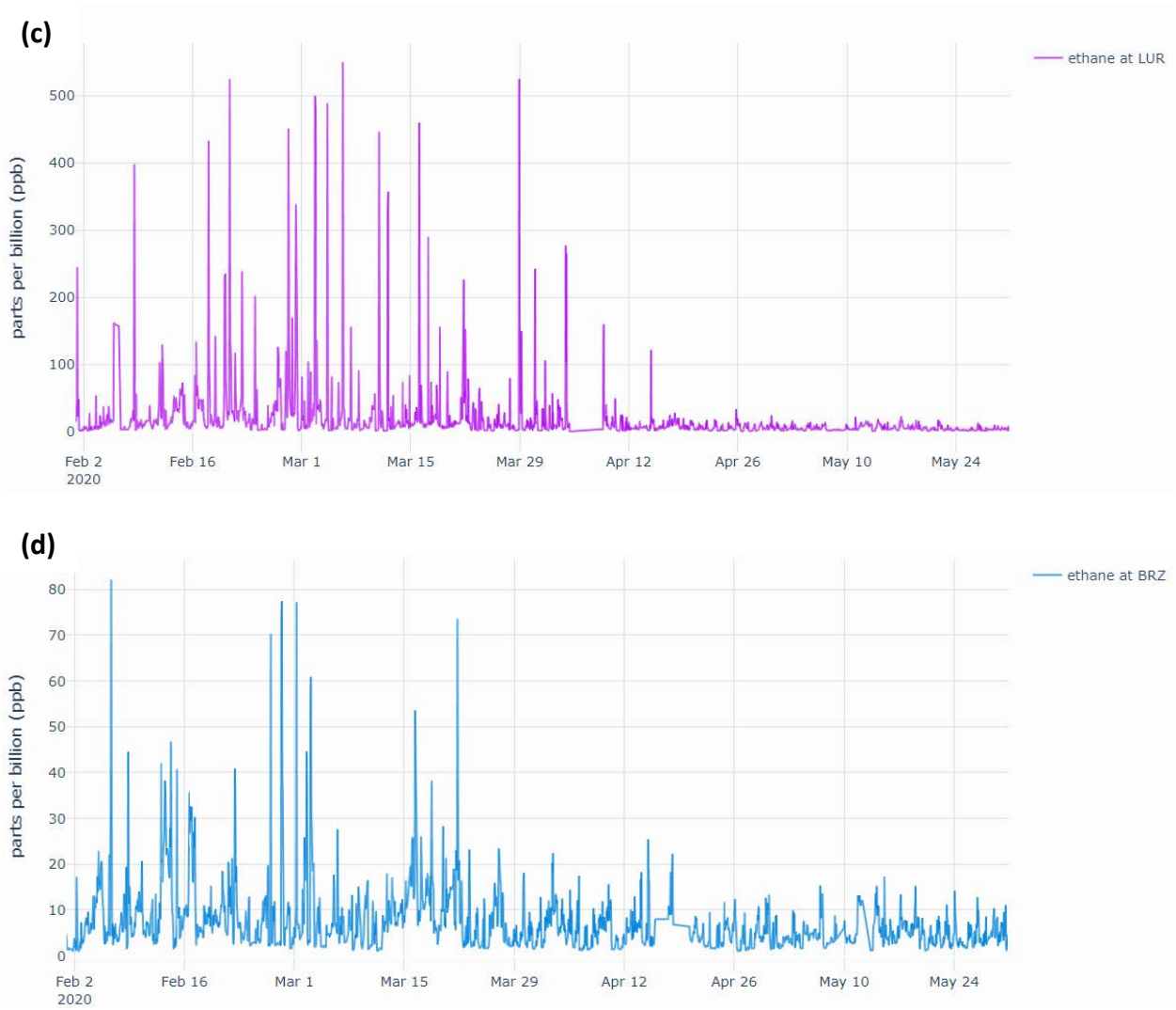

Figure 8 (continued):
Same ethane data as in Figure 8b, but with ethane at LUR (c) and BRZ (d) during February – May plotted as individual time series and the BRZ data scaled to 80 ppb to better illustrate the relative decline in the frequency and observed maximum levels at both sites.

(e)

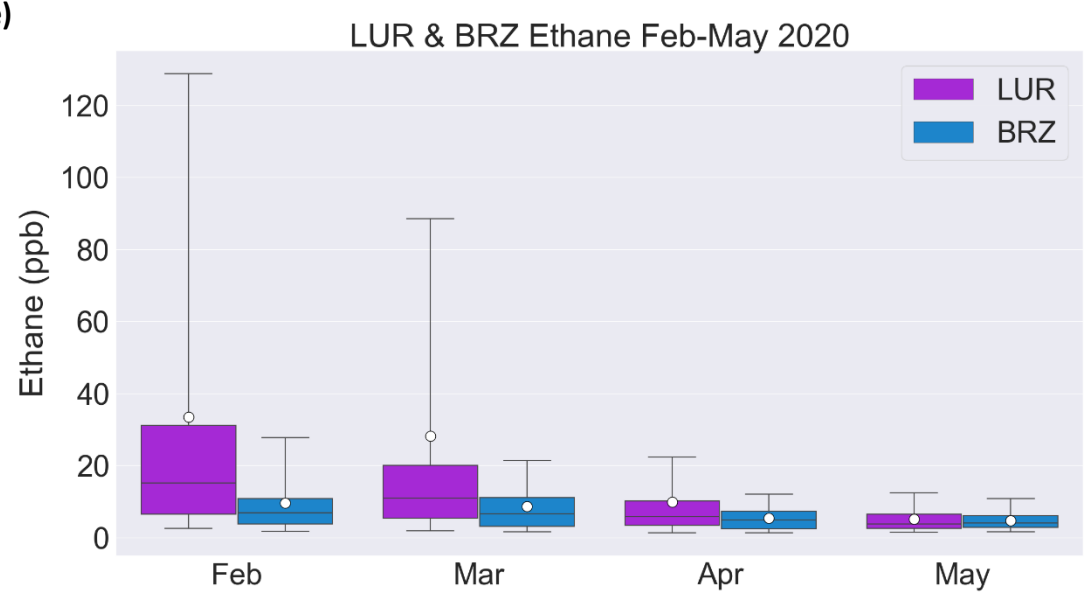

(f)

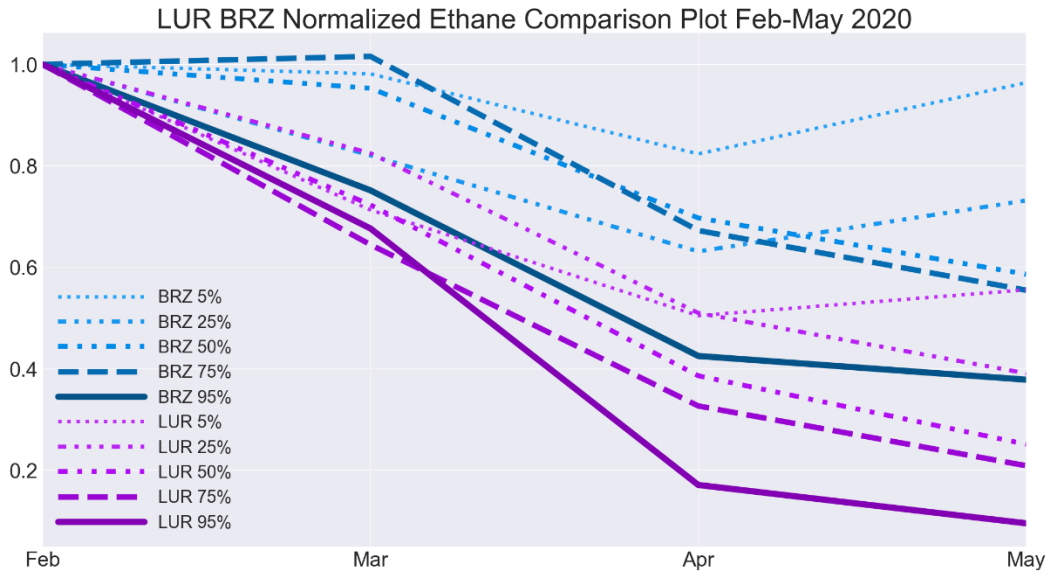

Figure 8 (continued):
(e) Same ethane data as in Figure 8 (a), binned into monthly increments and analyzed for the statistical distribution in box-whisker plots. (f) The percentile values from the box whisker plots in (e) normalized to the February values to show the differences in the decline rates between the two sites. The decline in ethane was much larger at LUR, and the difference was larger at the higher percentiles, becoming progressively smaller towards the lower percentile values.

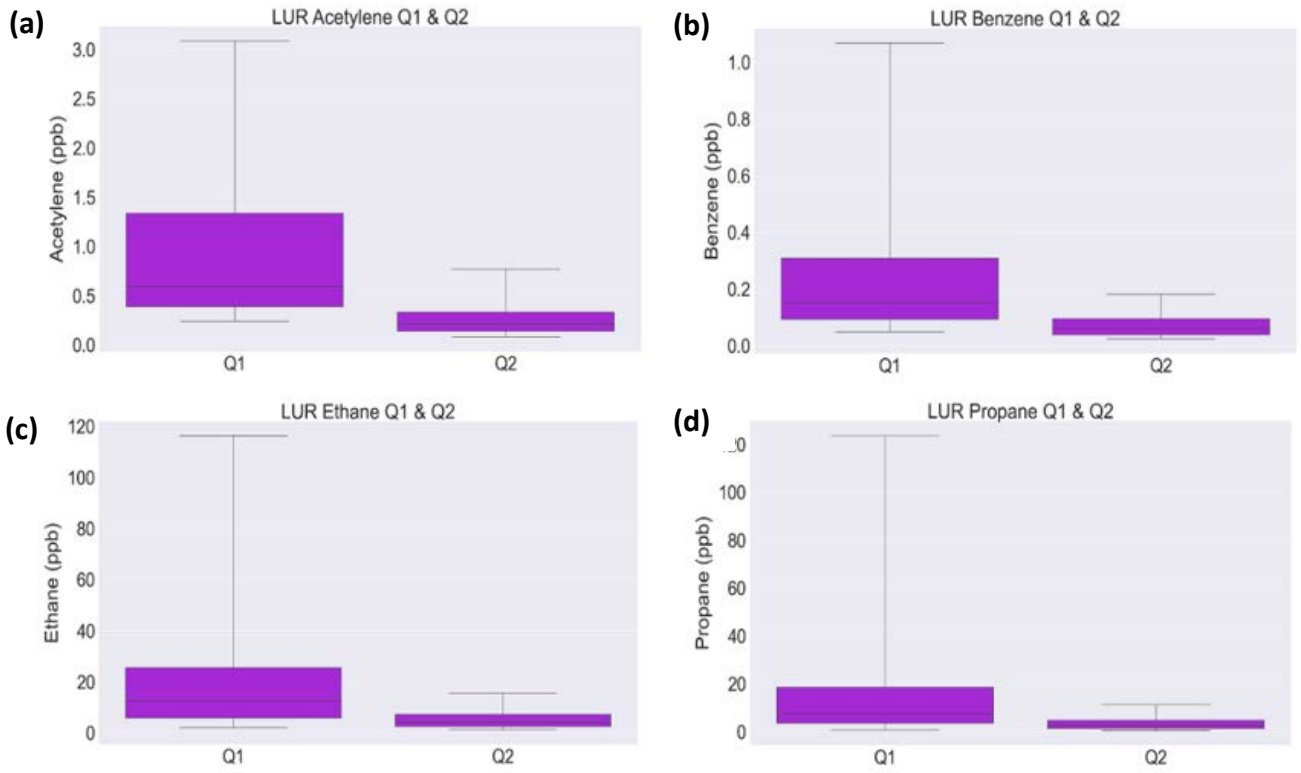

Figure 9:
Comparison of the distribution of acetylene (a), benzene (b), ethane (c), and propane (d) at LUR during Q1 and Q2. All VOCs had a lower variability and lower percentile values during Q2. Please note that Q1 data are for February to March only. See Figure 1 for explanation of the box and whisker plot formats.

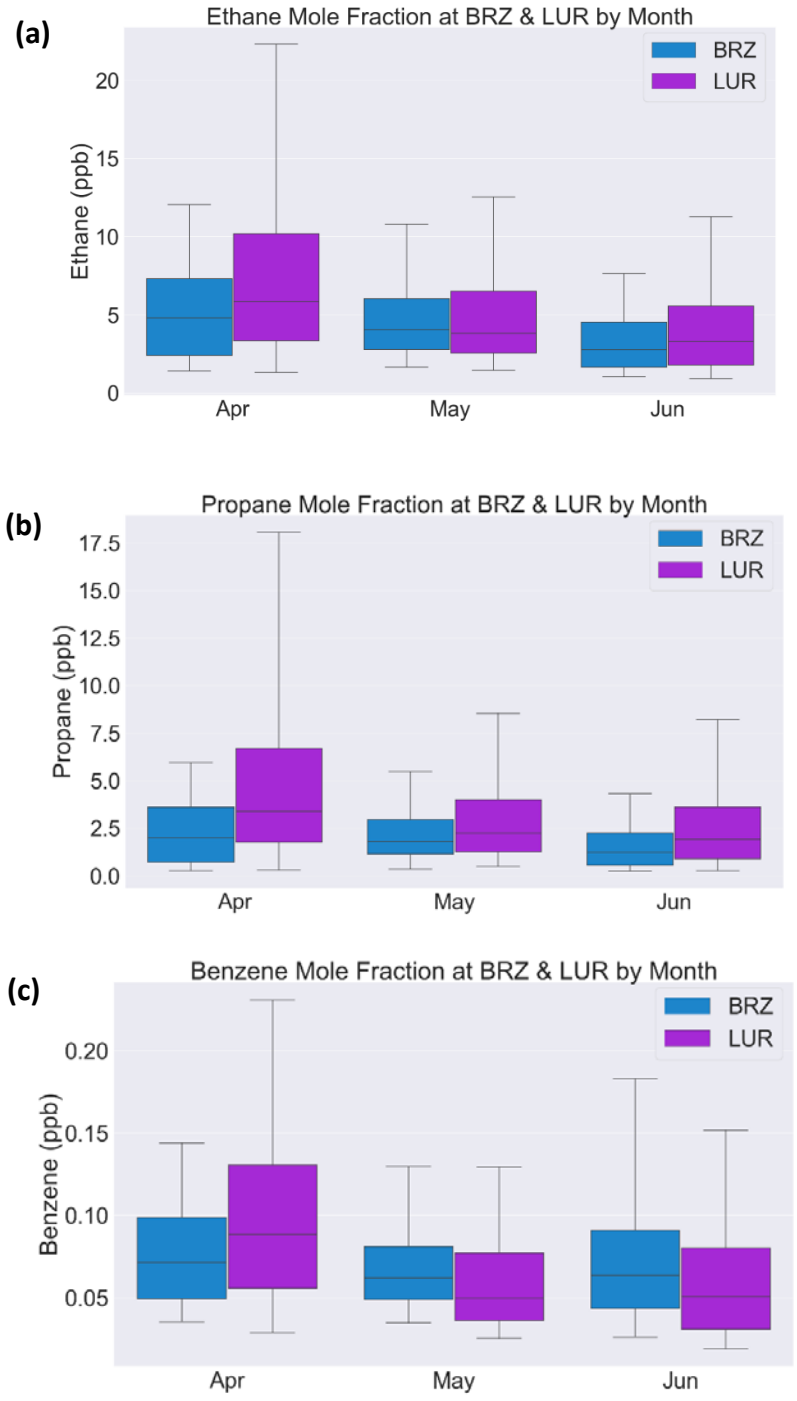

Figure 10:
Comparison of the distribution of ethane (a), propane (b), and benzene (c) at BRZ and LUR during Q2. Levels were higher at LUR, though the magnitude of the difference became smaller towards the latter part of the quarter. For benzene, the order reversed in May and June, when overall slightly higher values were measured at BRZ. See Figure 1 for explanation of the box and whisker plot formats.

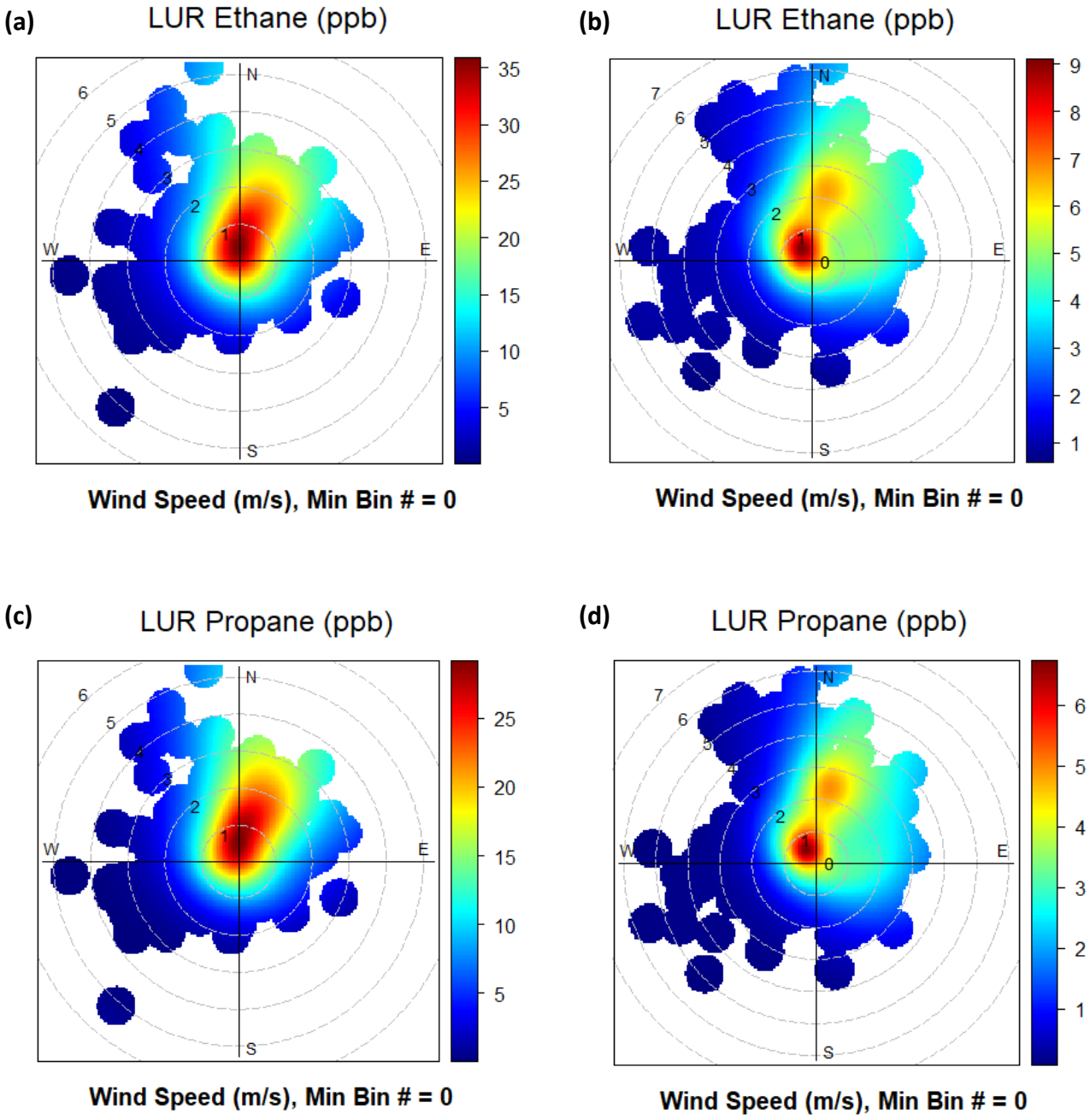

Figure 11a
Comparison of ethane (top) and propane (right) occurrences as a function of wind speed and direction at LUR during Q1 (left), and Q2 (right). Note the difference scales of the concentration color scales between the Q1 and Q2 data. The strong predominance of transport with elevated levels from the northeast sector was weaker in Q2. The Min Bin number is a filter that is used on occasion to reject data bins that have a low number of data. In this case, with Min Bin # = 0, no bins were rejected.

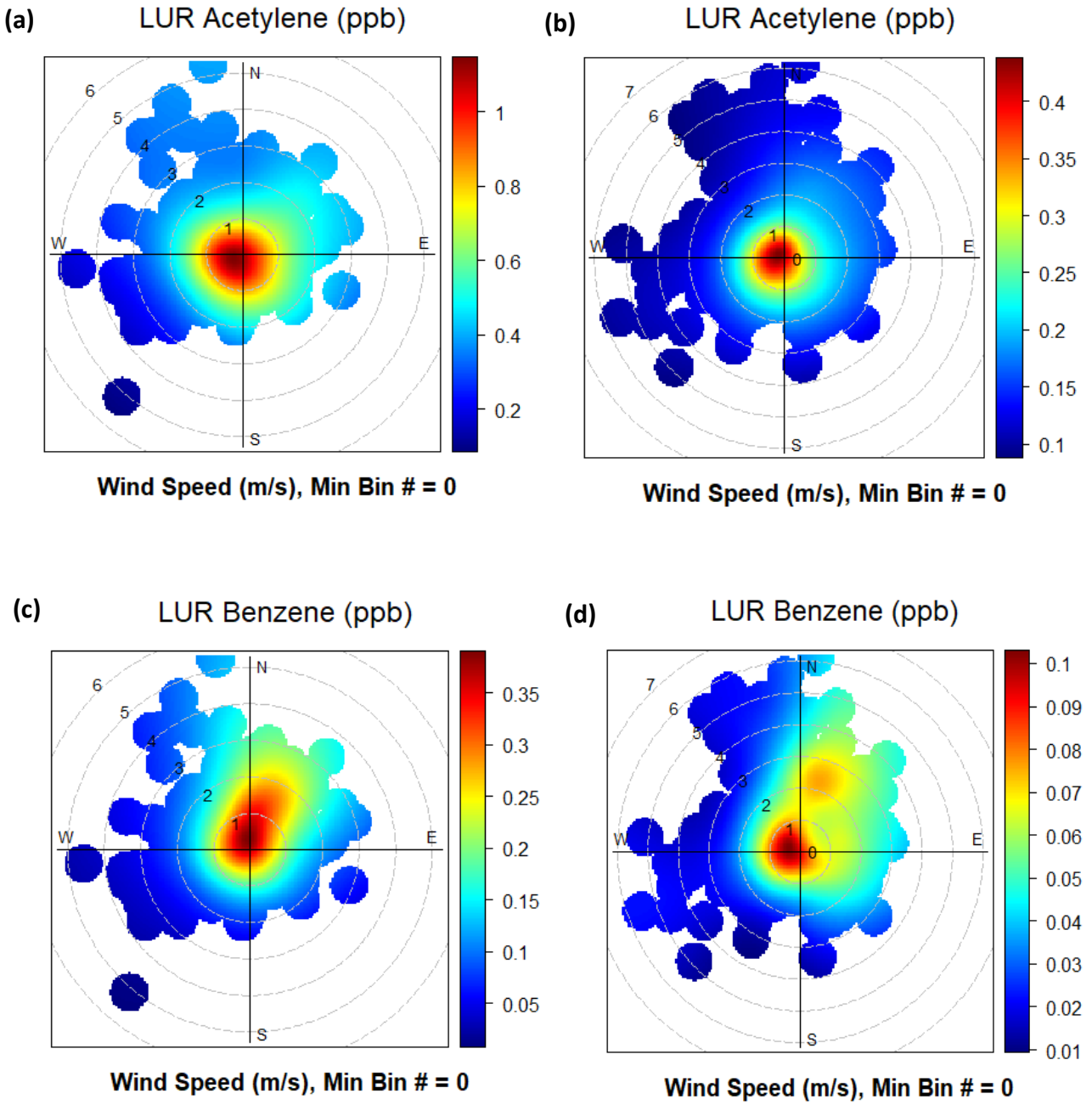

Figure 11b:
Same as Figure 11a for acetylene (top) and benzene (bottom), with again Q1 data on the left, and Q2 data on the right. Note the difference scales of the concentration color scales between the Q1 and Q2 data. Acetylene shows slightly higher values in transport from the west. The clear dominance of a strong benzene source in the northeast sector diminished during Q2. The Min Bin number is a filter that is used on occasion to reject data bins that have a low number of data. In this case, with Min Bin # = 0, no bins were rejected.

Figure 12:
Wind direction during the ten largest benzene peaks during Q2. The arrows indicate the direction that the wind was coming from during the time window when the benzene peak was detected. The majority of high benzene occurrences was associated with transport from the northwest to northeast sectors.

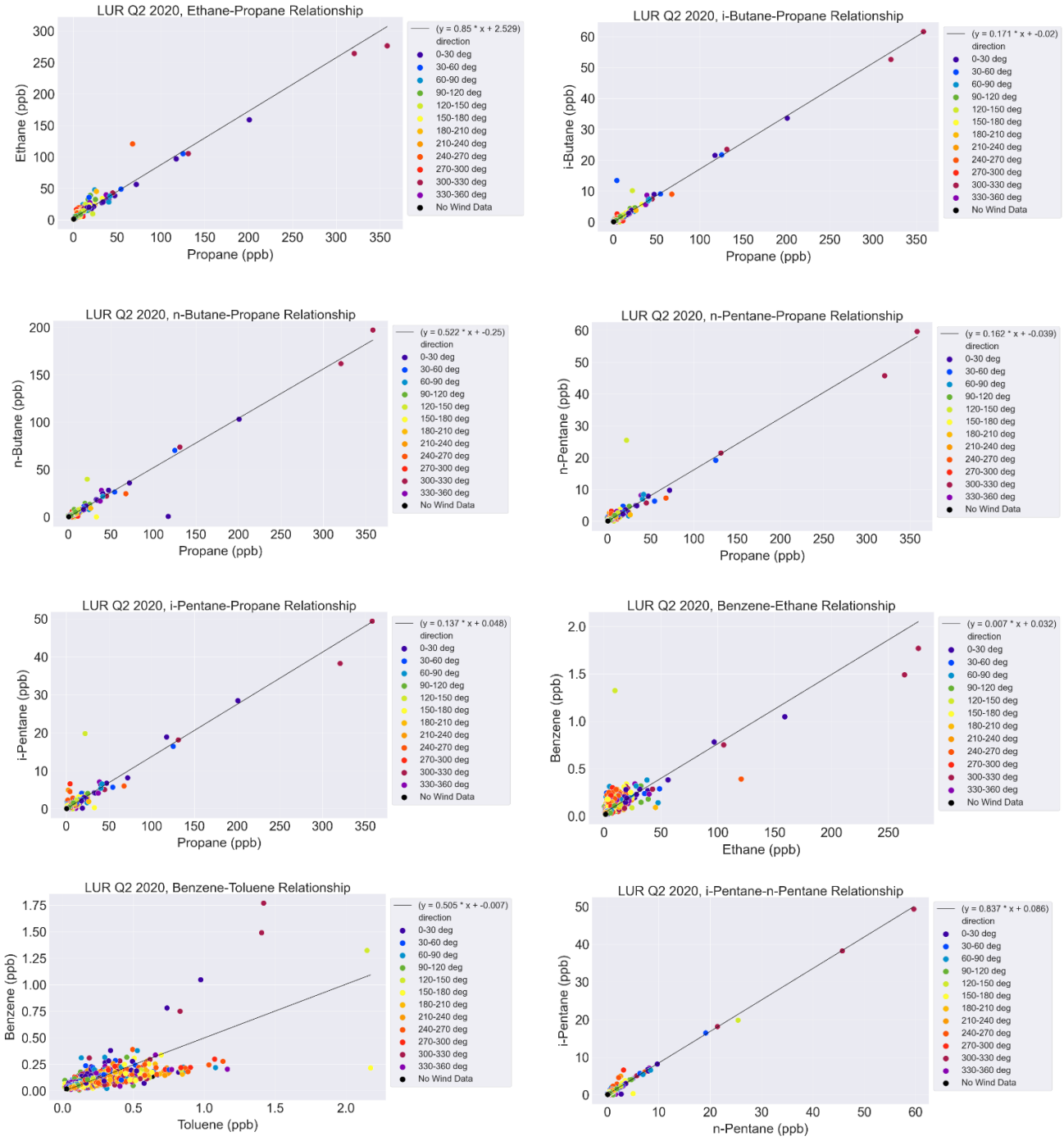

Figure 13:
Correlation between pairs of VOCs at LUR during Q2. Data points are color coded by wind direction as indicated in the legend. The black line is the result of an orthogonal (linear two-sided) best regression fit calculation.

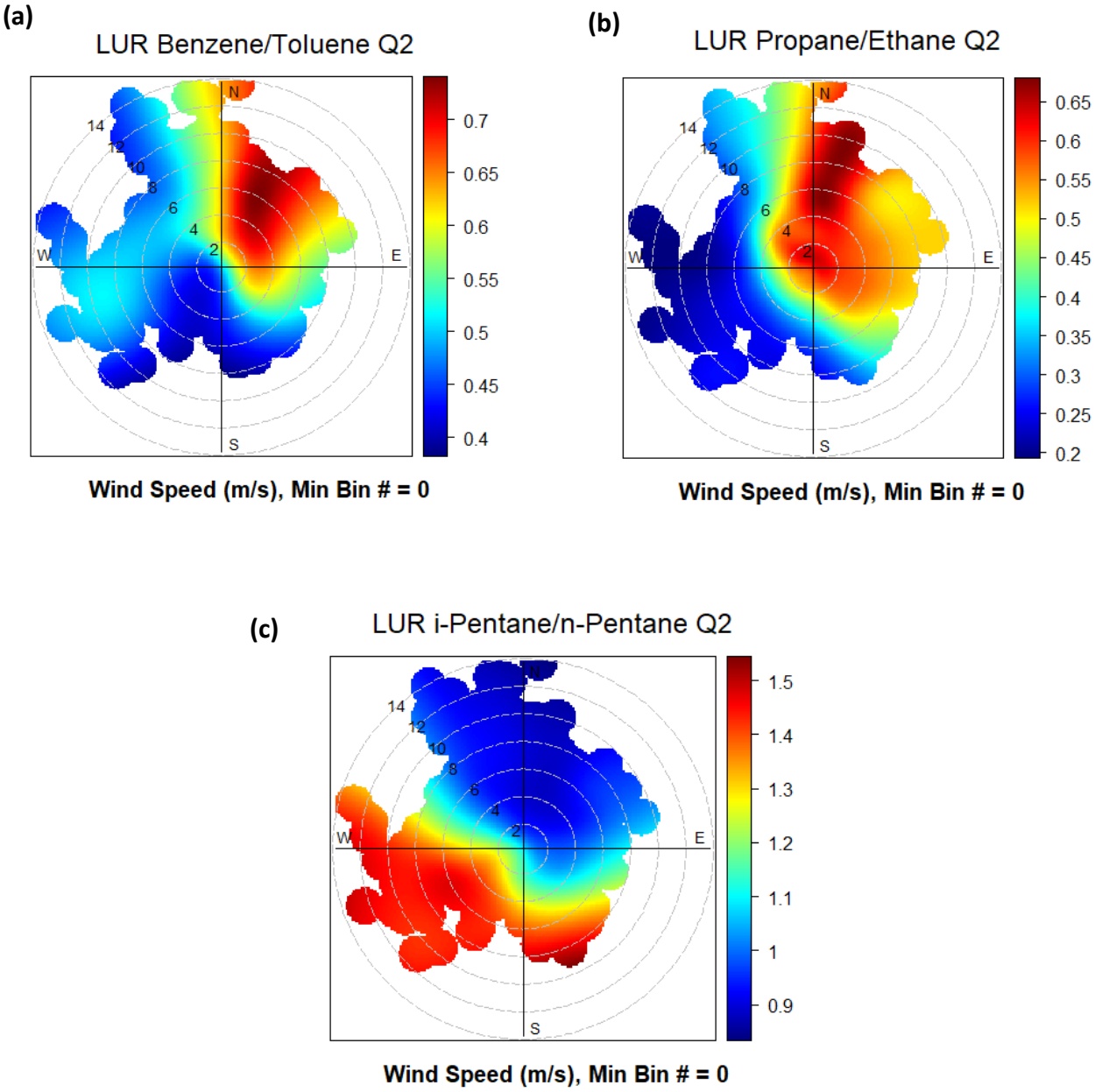

Figure 14:
Ratios of selected VOC pairs as a function of wind direction and wind speed. The Min Bin number is a filter that is used on occasion to reject data bins that have a low number of data. These graphs show the stark difference in the relative VOCs composition depending on air transport direction. In these cases, with Min Bin # = 0, no bins were rejected.

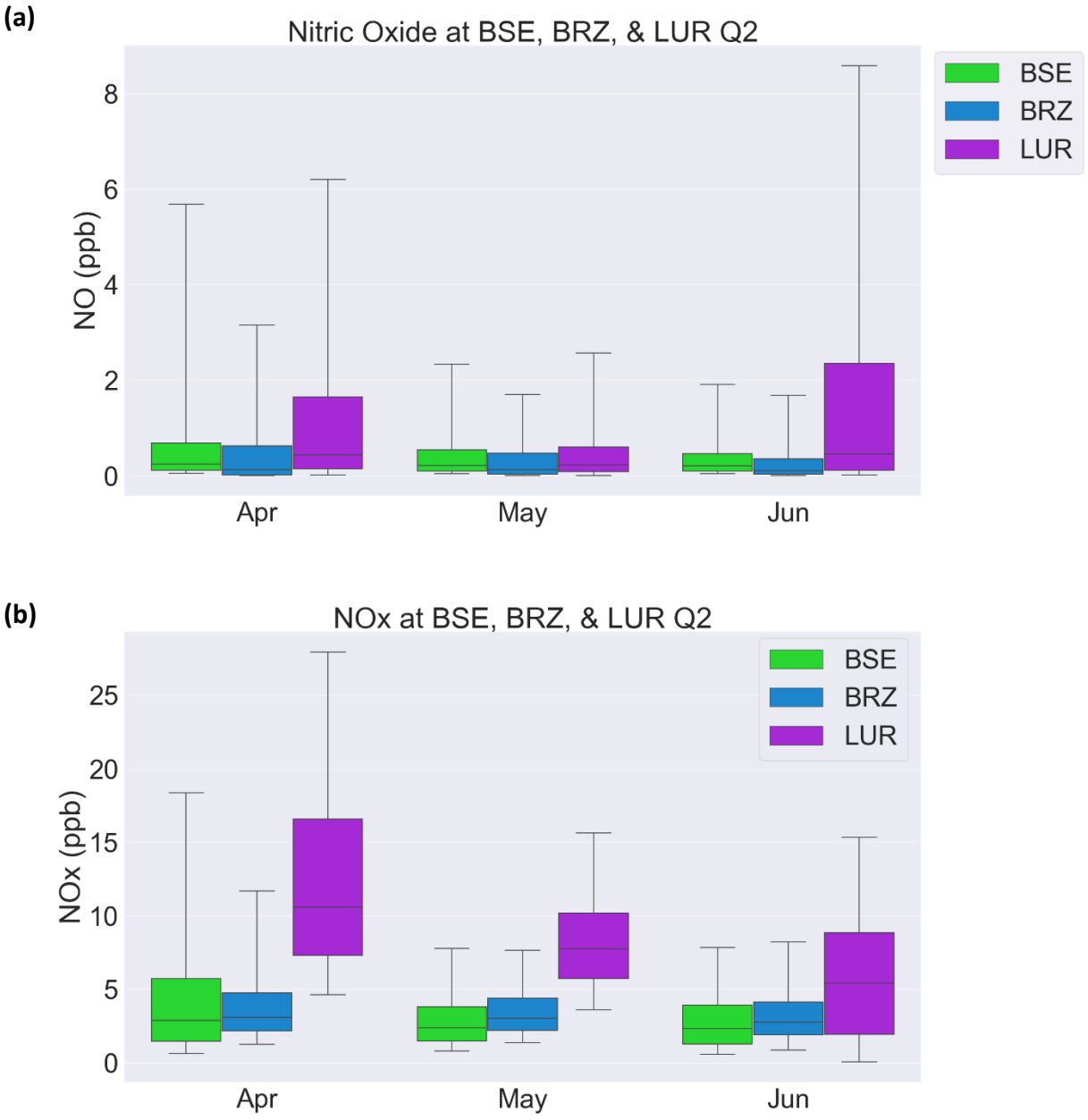

Figure 15:
Comparison of nitric oxide (a) and nitrogen oxides (b) at BSE, BRZ, and LUR during April – June 2020. LUR is clearly the site with the highest variability and overall highest observed NO_x levels in this comparison. See Figure 1 for explanation of the box and whisker plot formats.

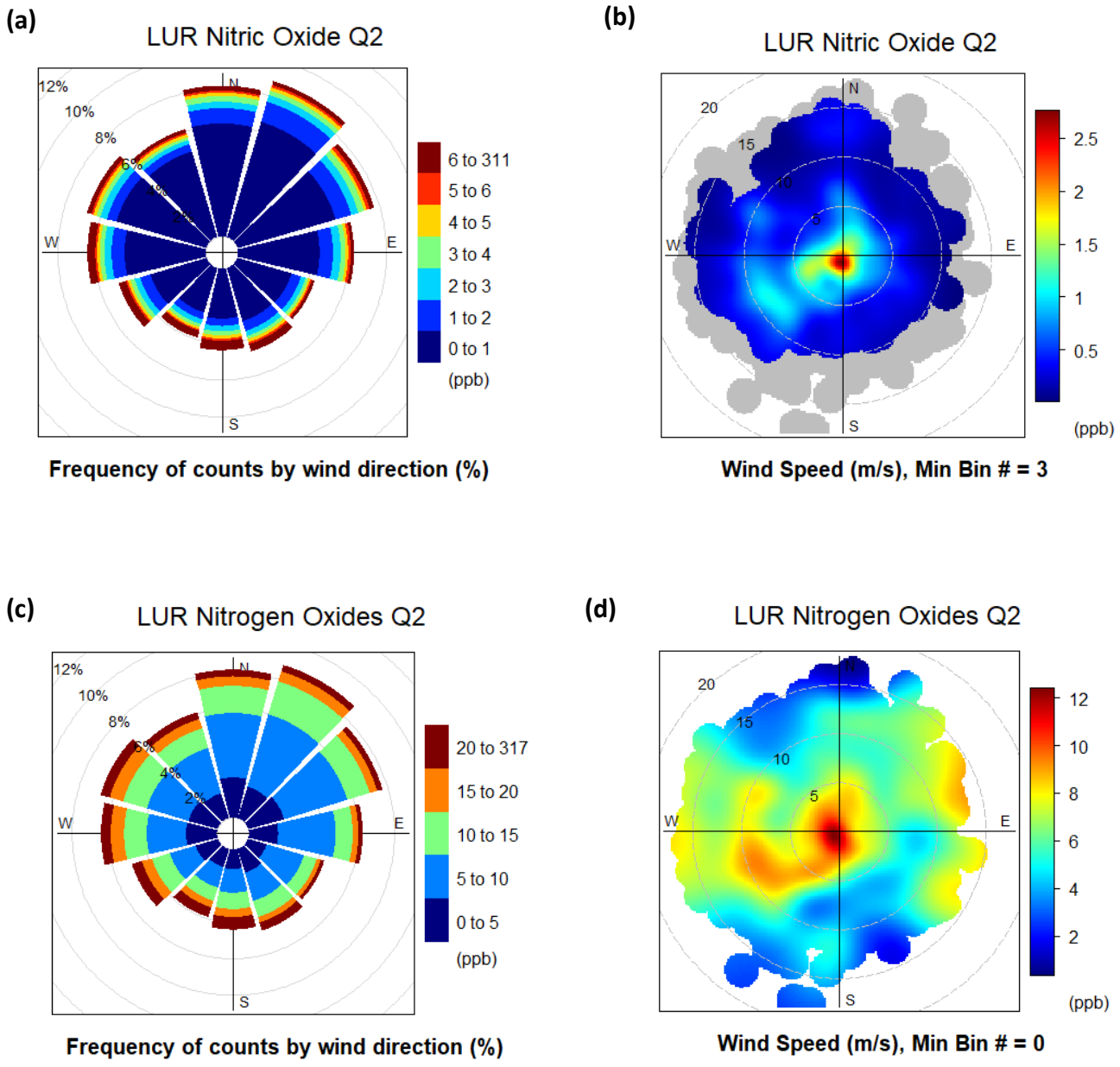

Figure 16:
Dependence of nitric oxide (top) and nitrogen oxides (bottom) as a function of wind speed and direction at LUR during April – June 2020. In contrast to methane and most VOCs, westerly sectors constitute the strongest NO_x source for this site. The Min Bin number is a filter that is used on occasion to reject data bins that have a low number of data.

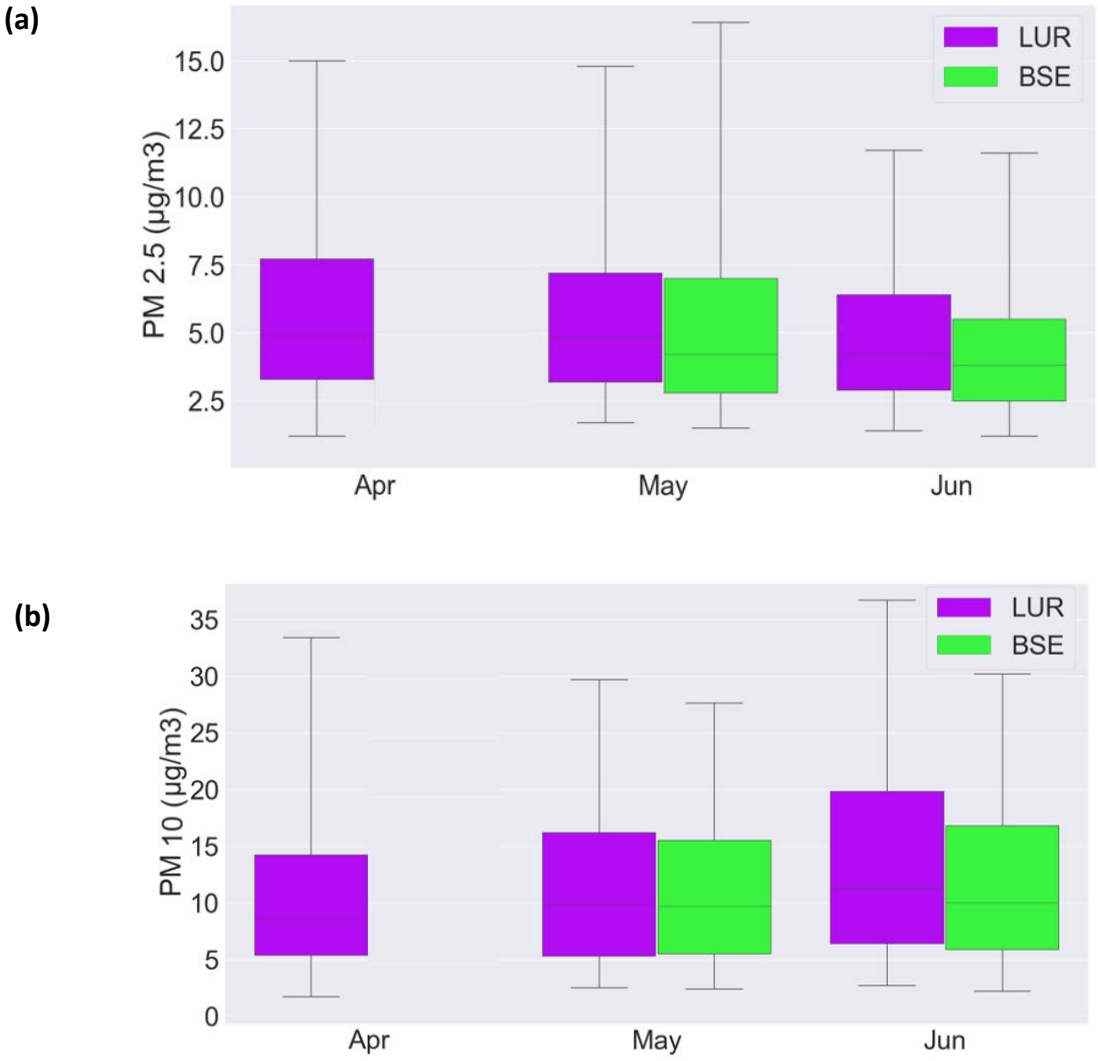

Figure 17:
Comparison of PM2.5 (a) and PM10 (b) mass concentrations at LUR and BSE during April – June 2020. Measurements at BSE were only available for part of the month of April and were therefore excluded from the April data comparison. PM levels are relatively similar between both sites. See Figure 1 for explanation of the box and whisker plot formats.

Supplement A

Preliminary Data LMA Quarter 1, 2020

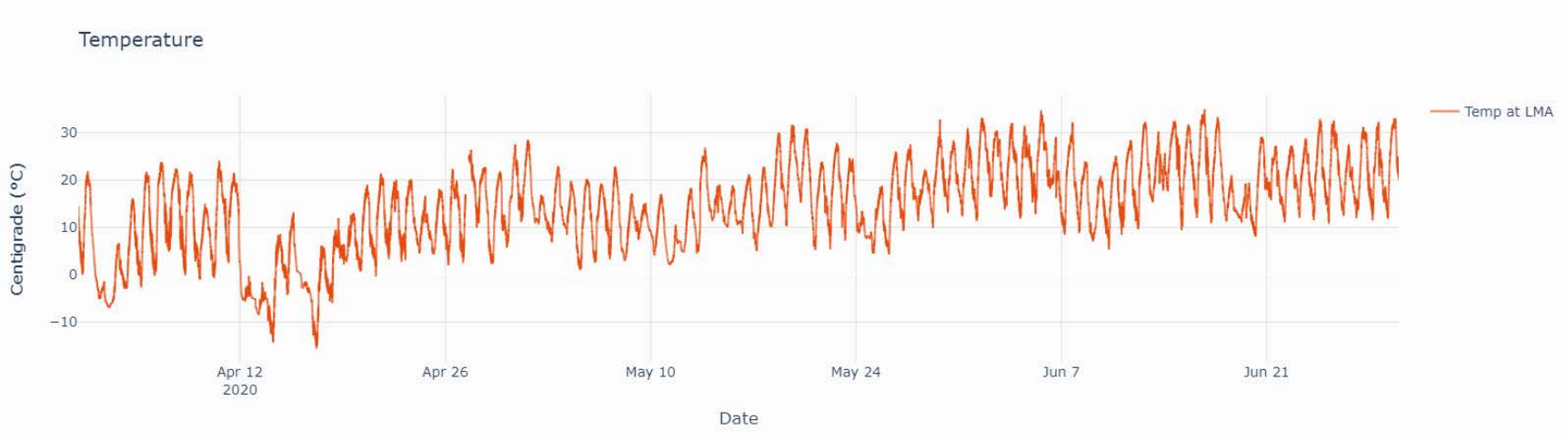

Figure SA1:
LMA temperature record April 1 – June 30, 2020.

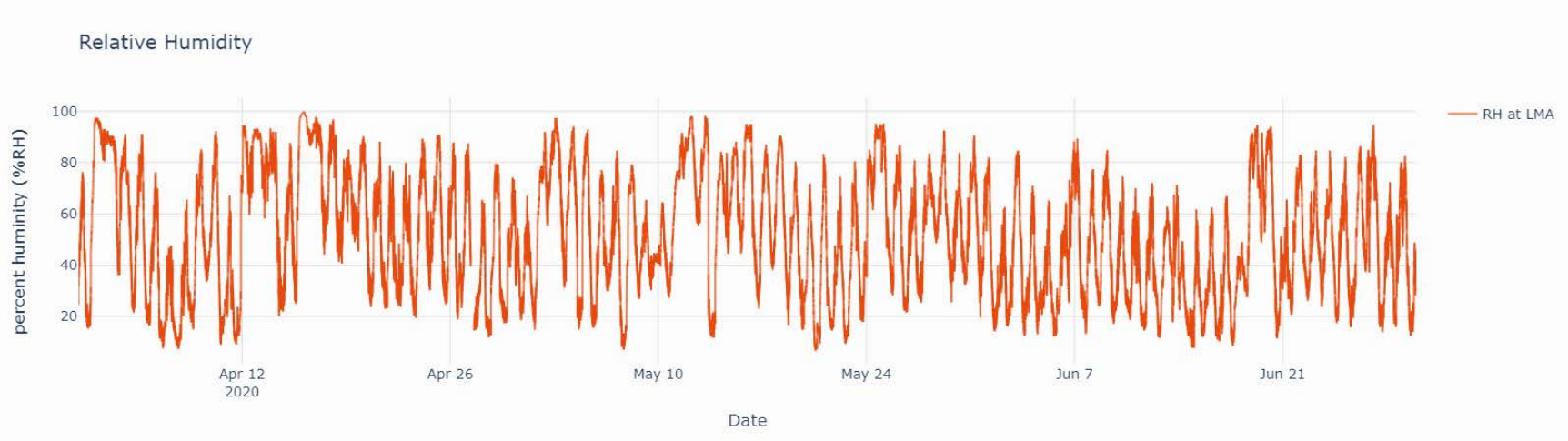

Figure SA2:
LMA humidity record April 1 – June 30, 2020.

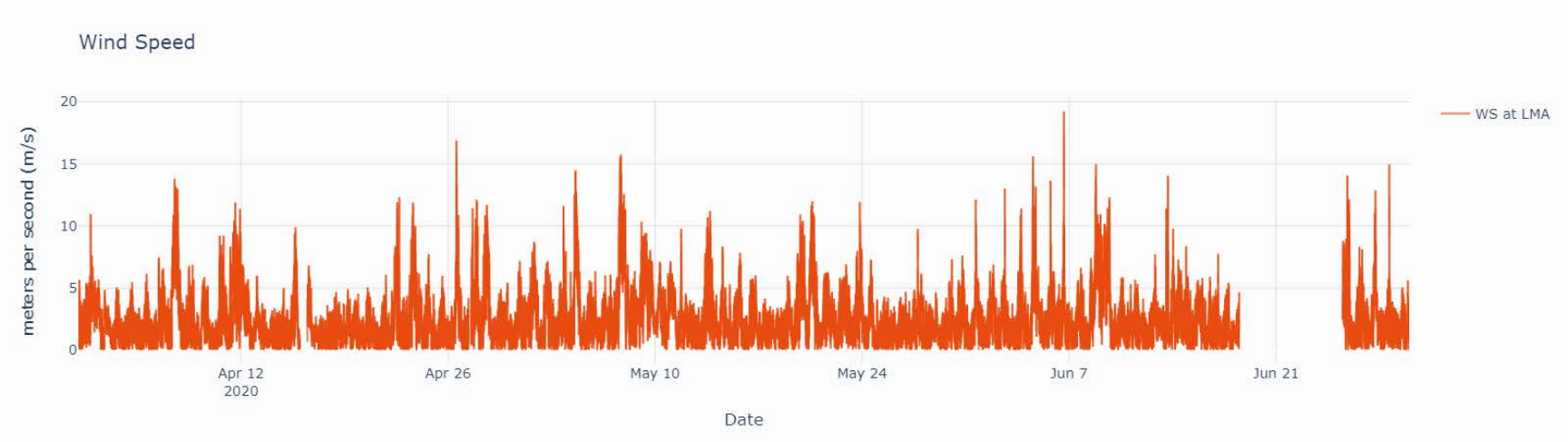

Figure SA3:
LMA wind speed record April 1 – June 30, 2020.

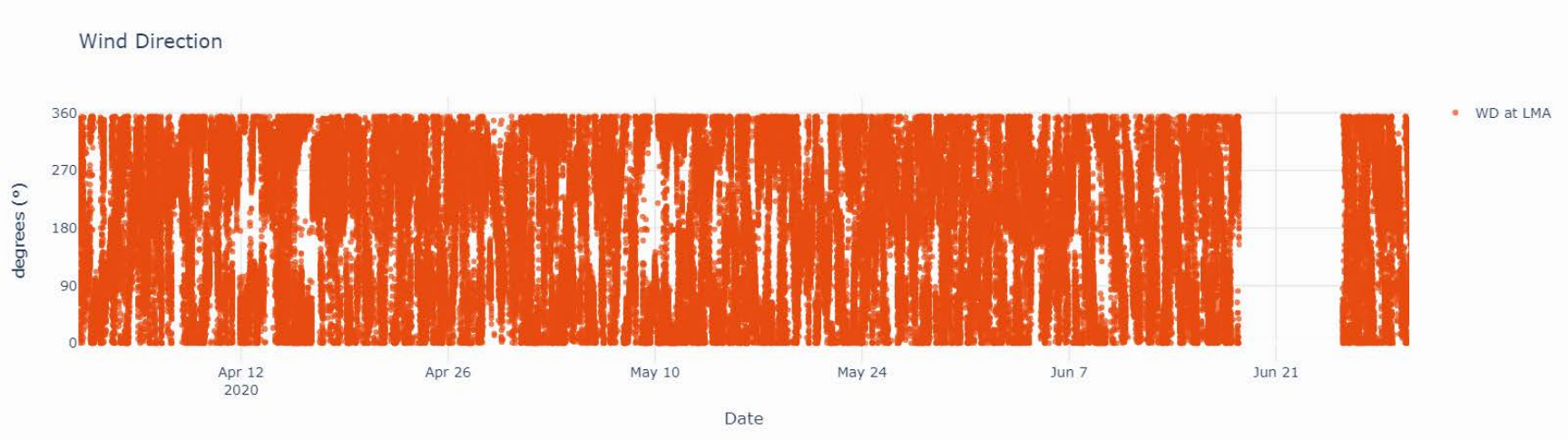

Figure SA4:
LMA wind direction record April 1 – June 30, 2020.

Figure SA5:
LMA solar radiation record April 1 – June 30, 2020.

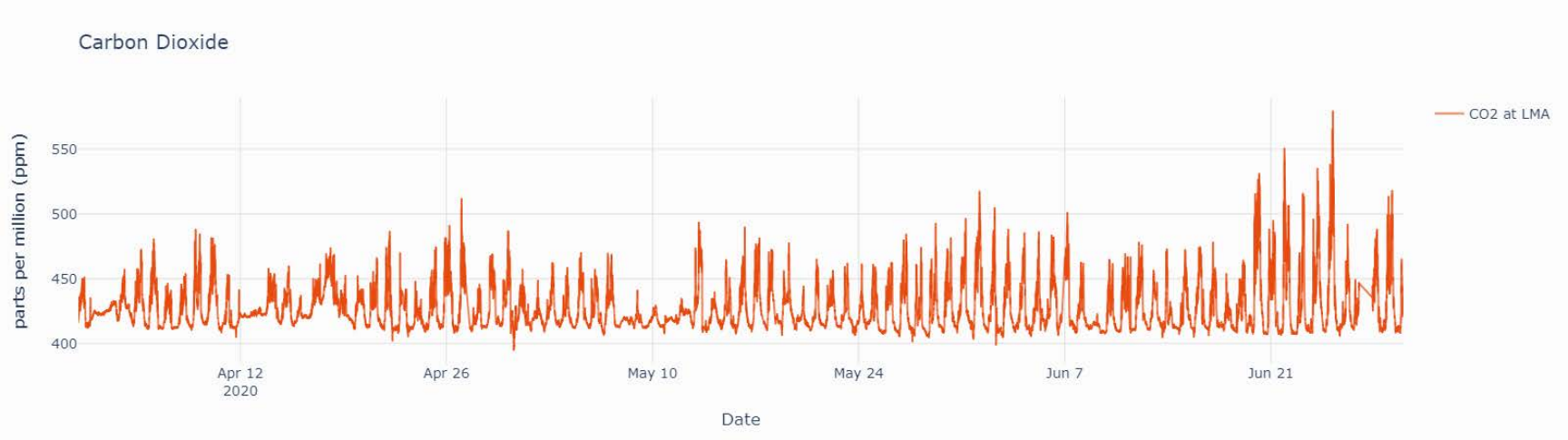

Figure SA6:
LMA CO_2 record January April 1 – June 30, 2020.

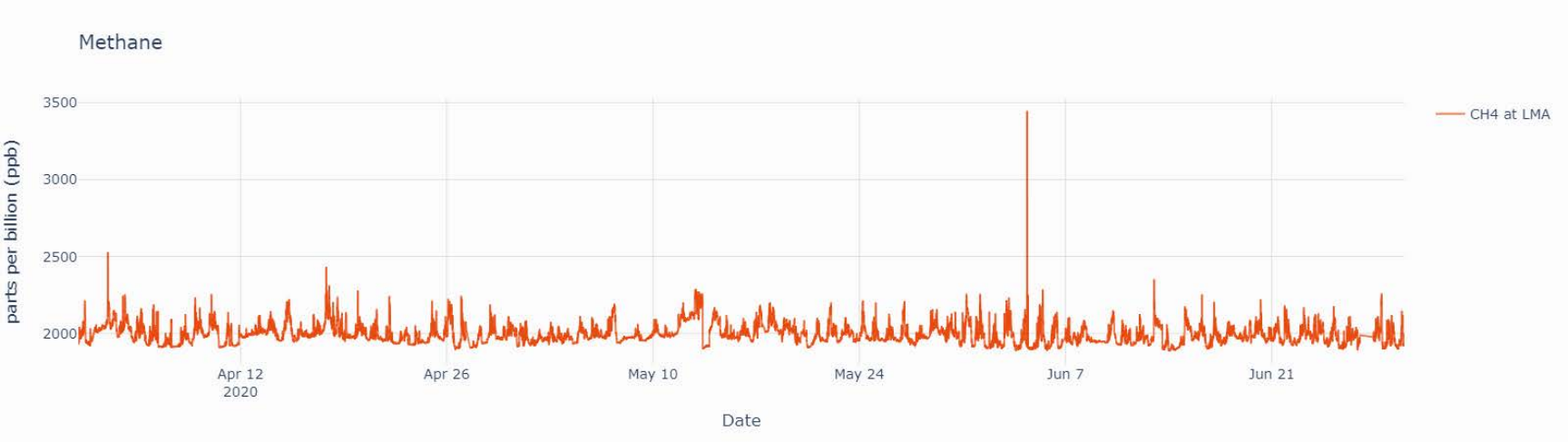

Figure SA7:
LMA methane record April 1 – June 30, 2020.

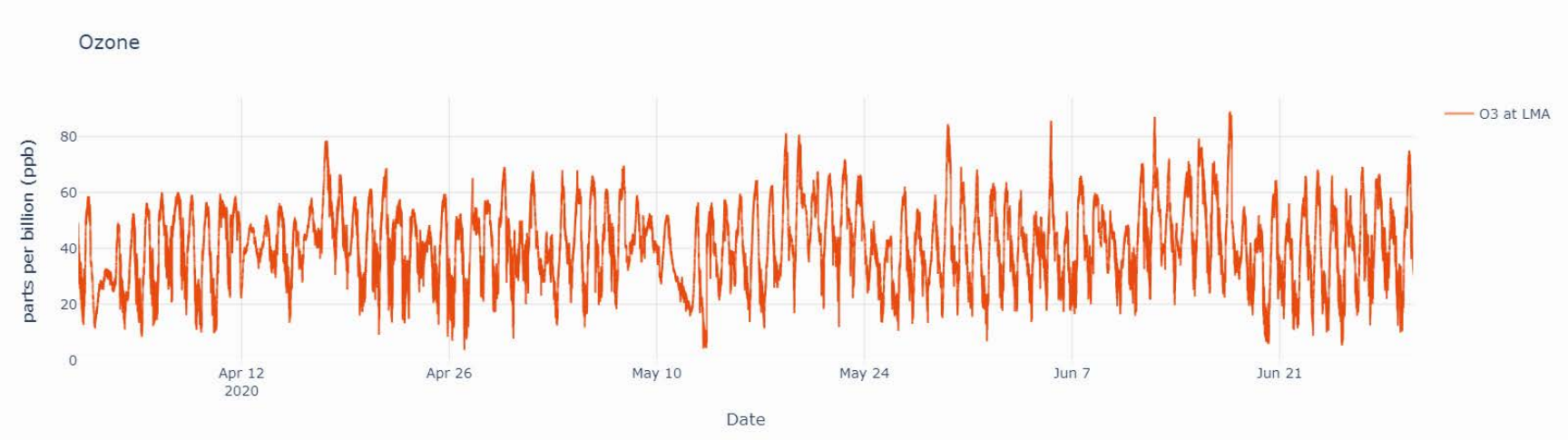

Figure SA8:
LMA ozone record April 1 – June 30, 2020.

Figure SA9:
LMA ozone 8-hour running average record April 1 – June 30, 2020.

Supplement B

Preliminary Data LUR 2020

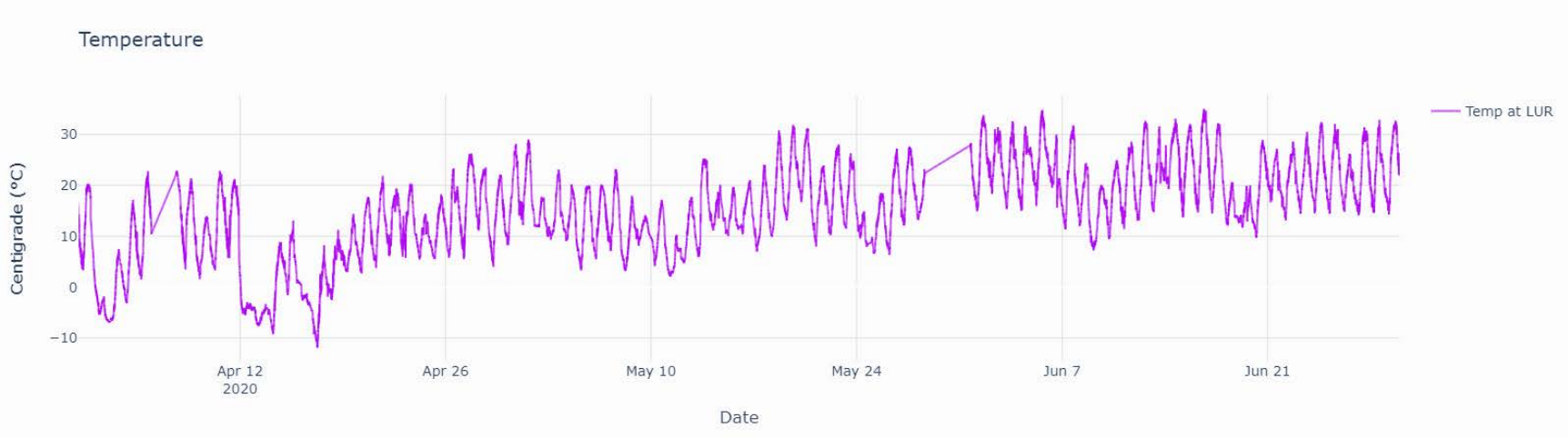

Figure SB1:
LUR temperature record April 1 – June 30, 2020.

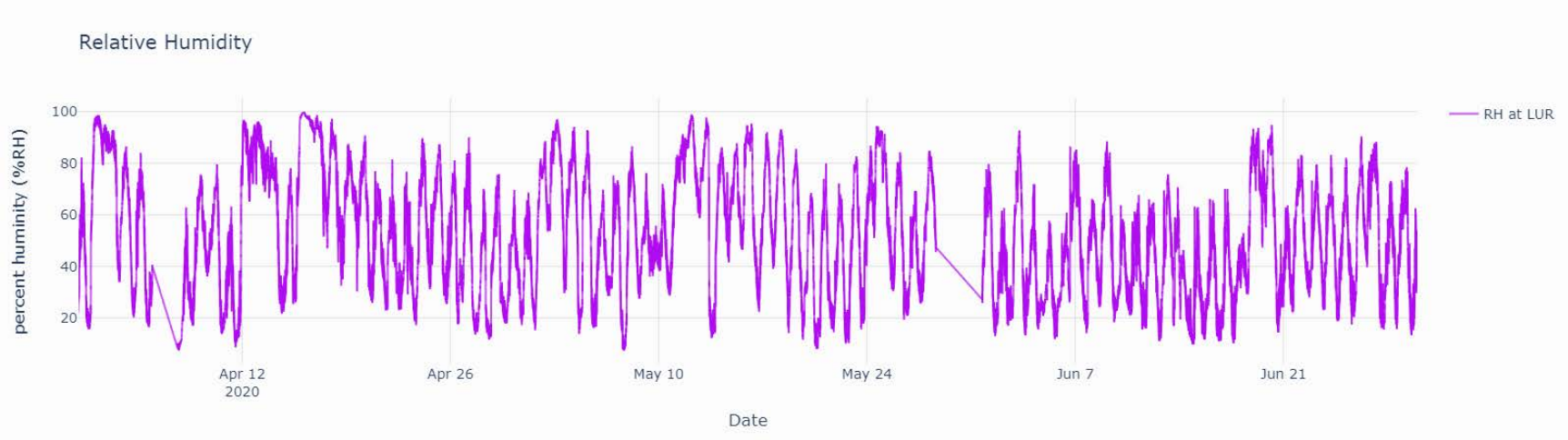

Figure SB2:
LUR humidity record April 1 – June 30, 2020.

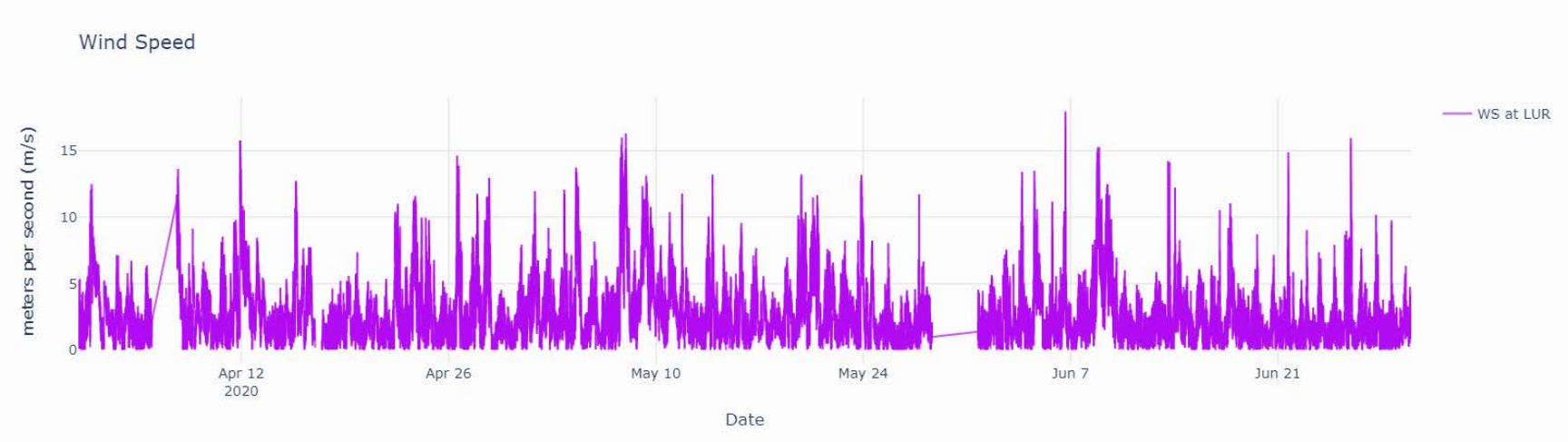

Figure SB3:
LUR wind speed record April 1 – June 30, 2020.

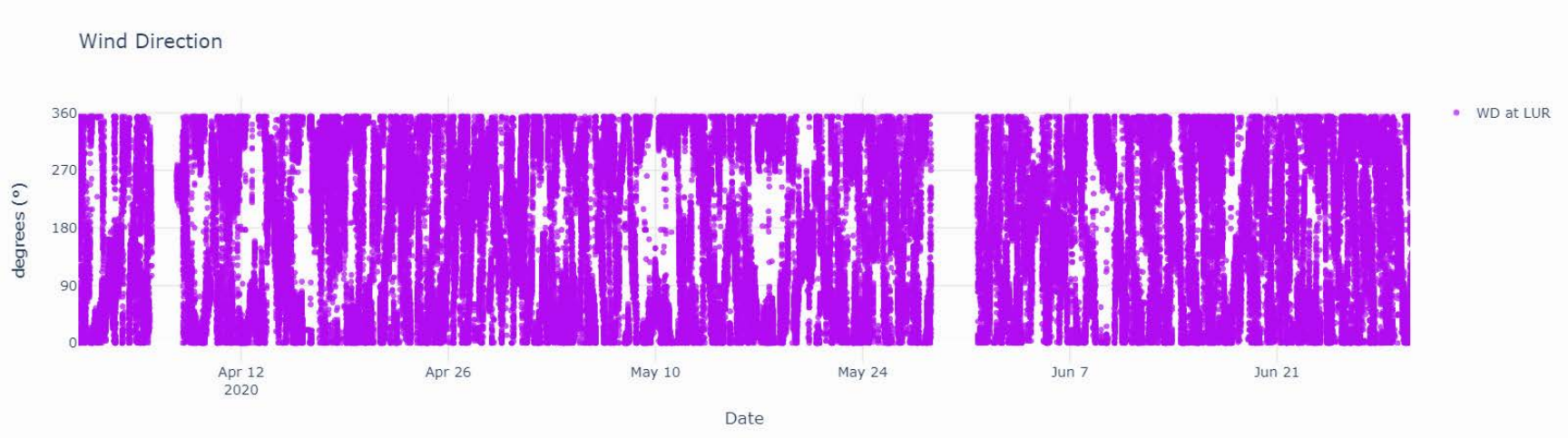

Figure SB4:
LUR wind direction record April 1 – June 30, 2020.

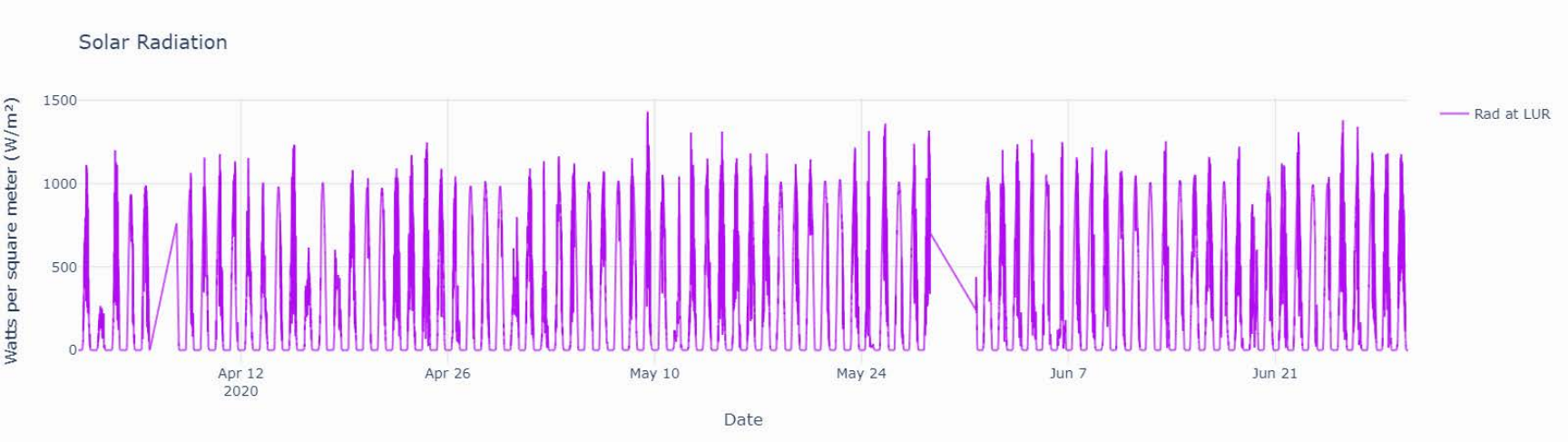

Figure SB5:
LUR solar radiation record April 1 – June 30, 2020.

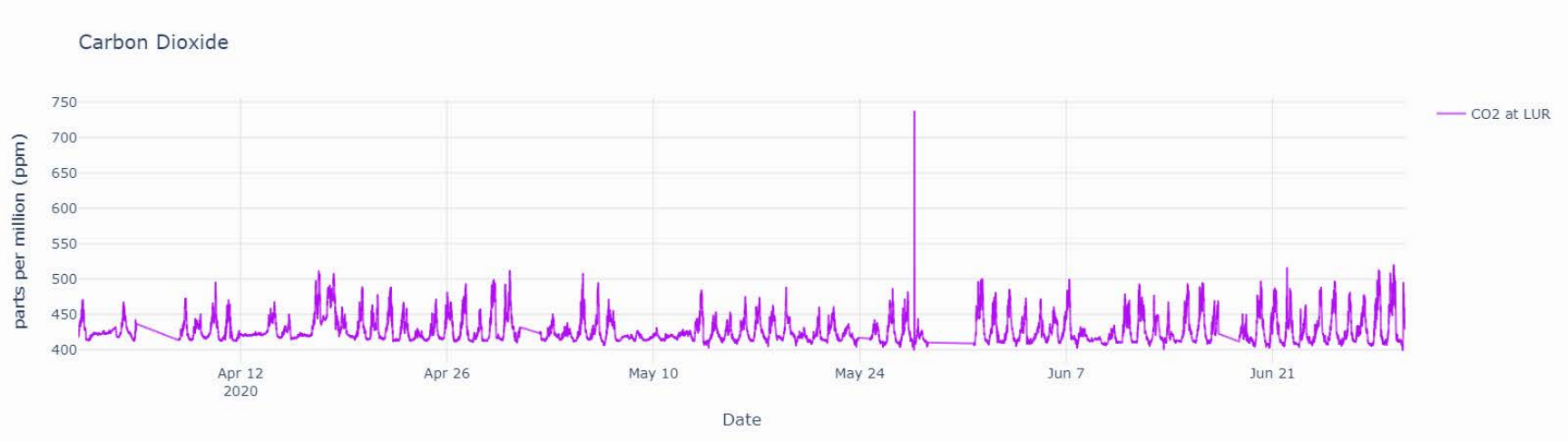

Figure SB6:
LUR CO_2 record April 1 – June 30, 2020.

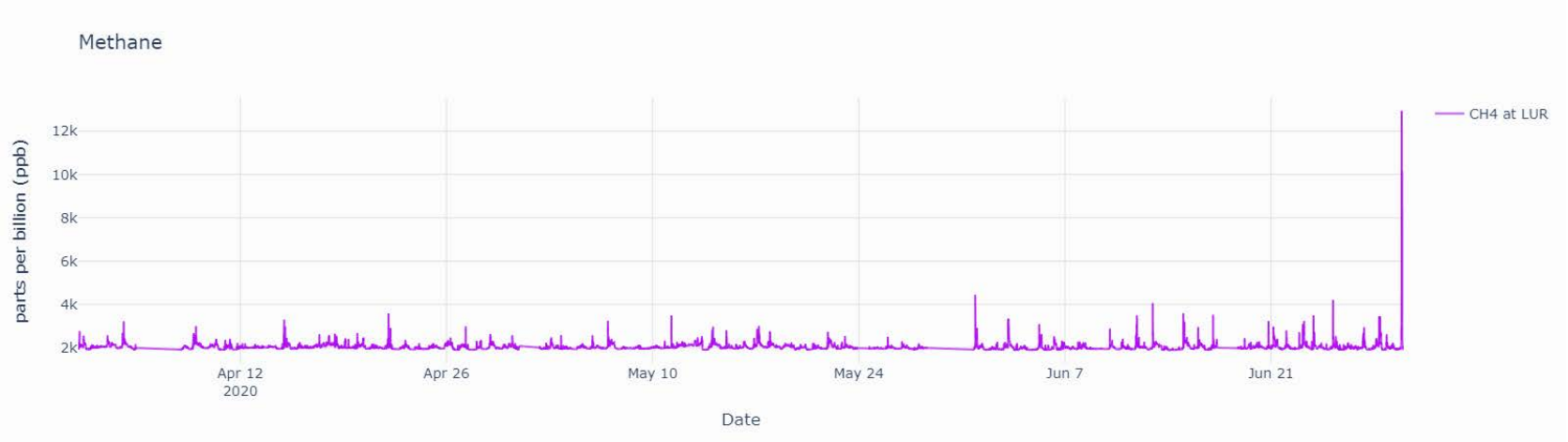

Figure SB7:
LUR methane record April 1 – June 30, 2020.

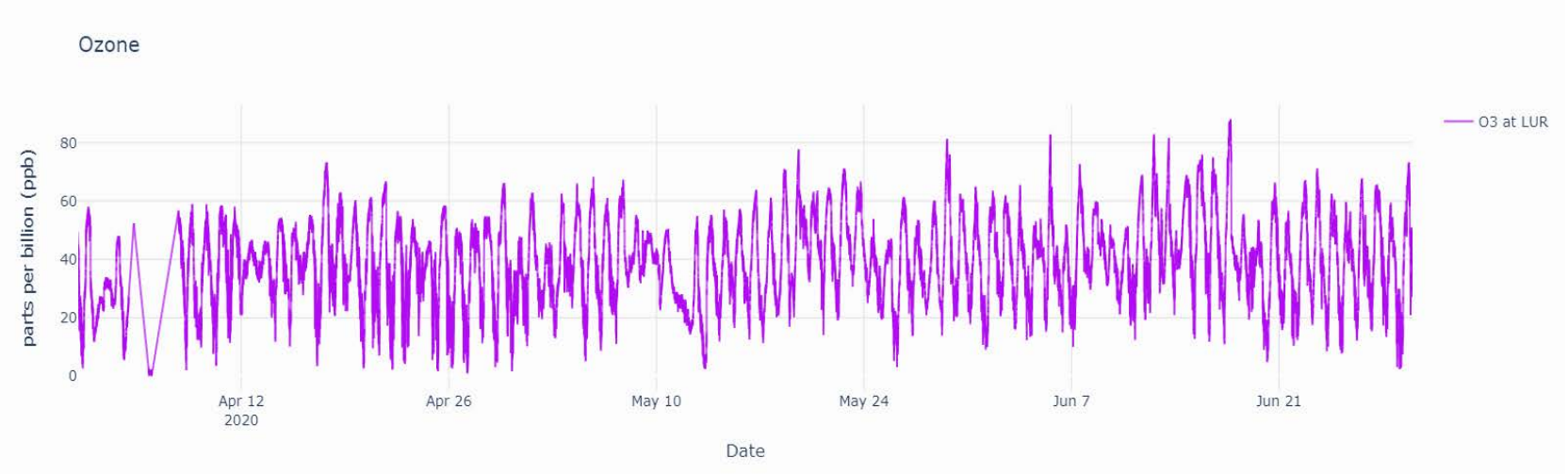

Figure SB8:
LUR ozone record April 1 – June 30, 2020.

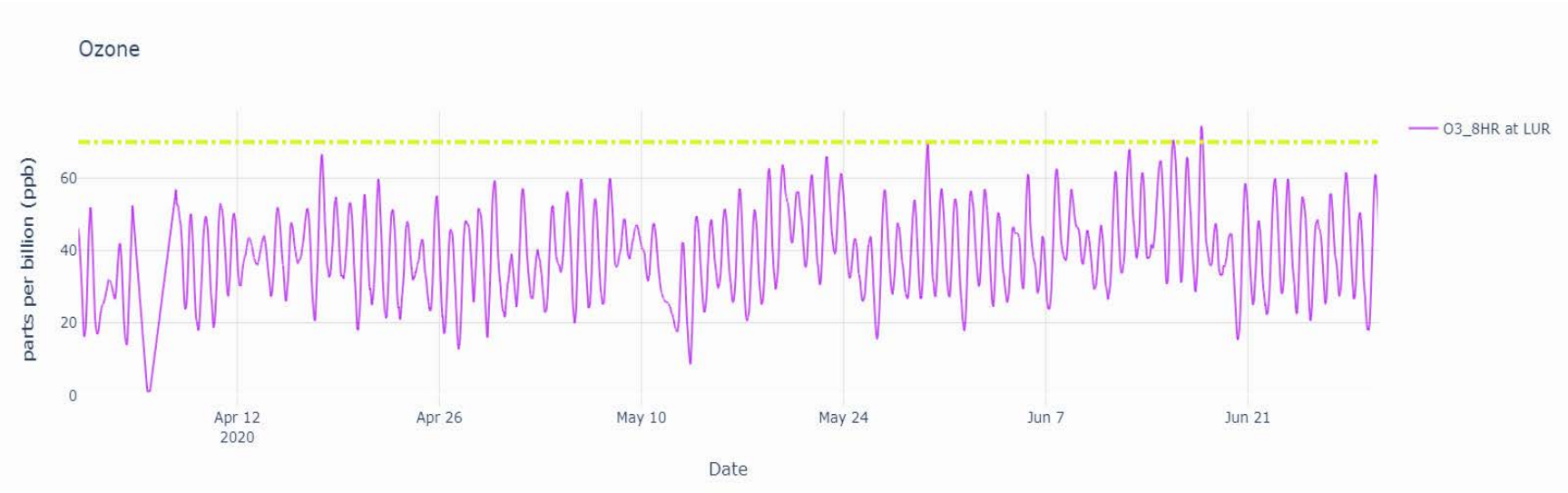

Figure SB9:
LUR ozone 8-hour running average record April 1 – June 30, 2020.

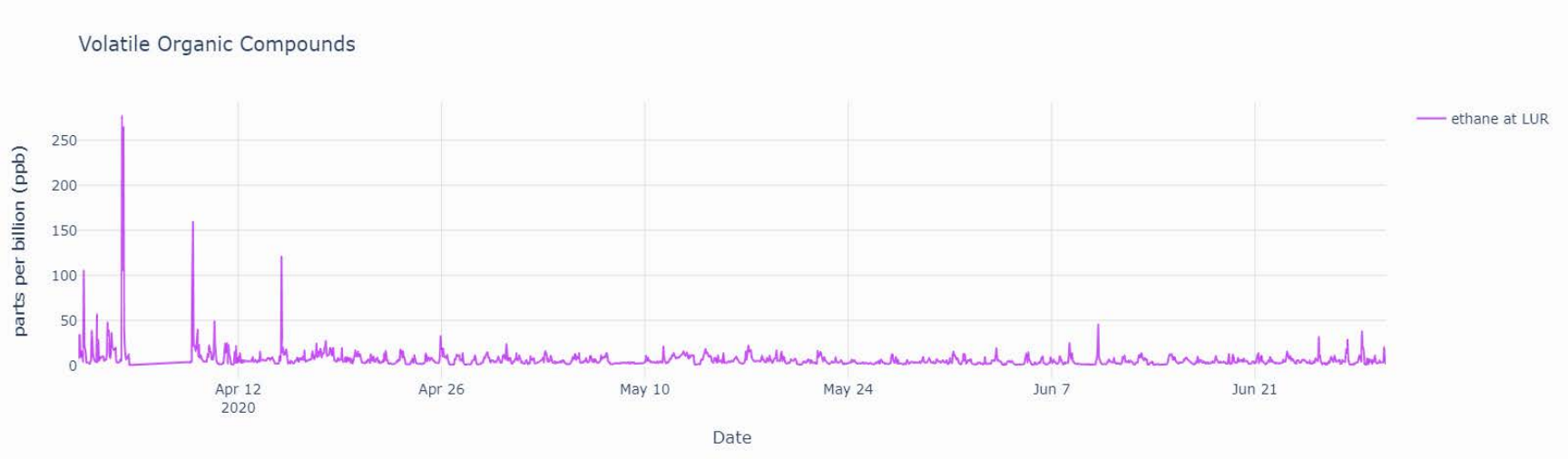

Figure SB10:
LUR ethane record April 1 – June 30, 2020.

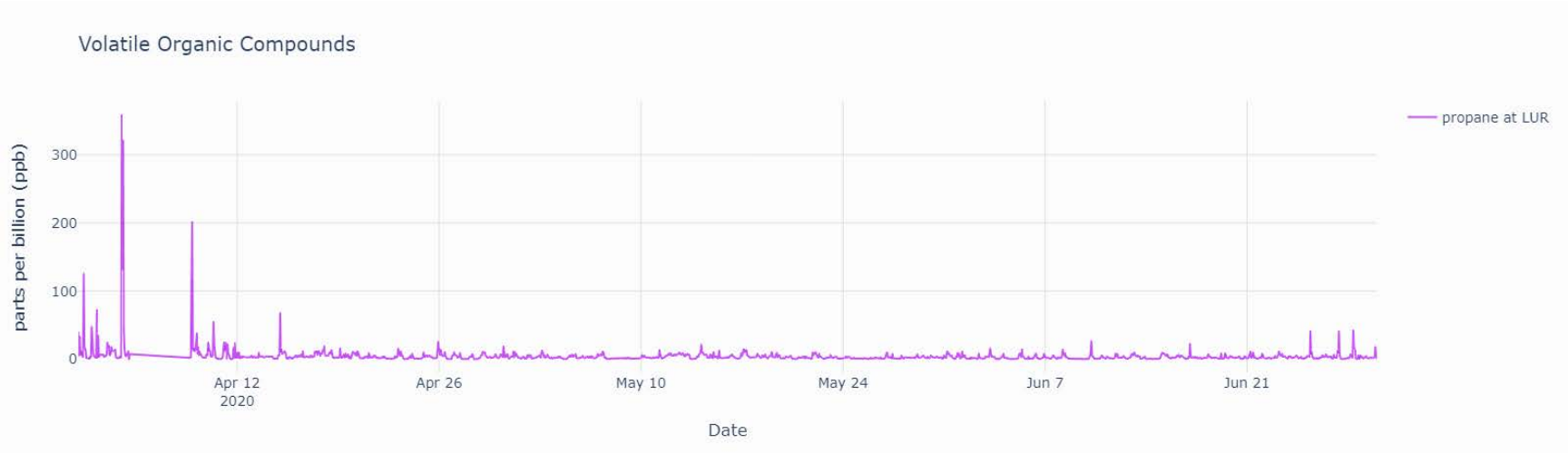

Figure SB11:
LUR propane record April 1 – June 30, 2020.

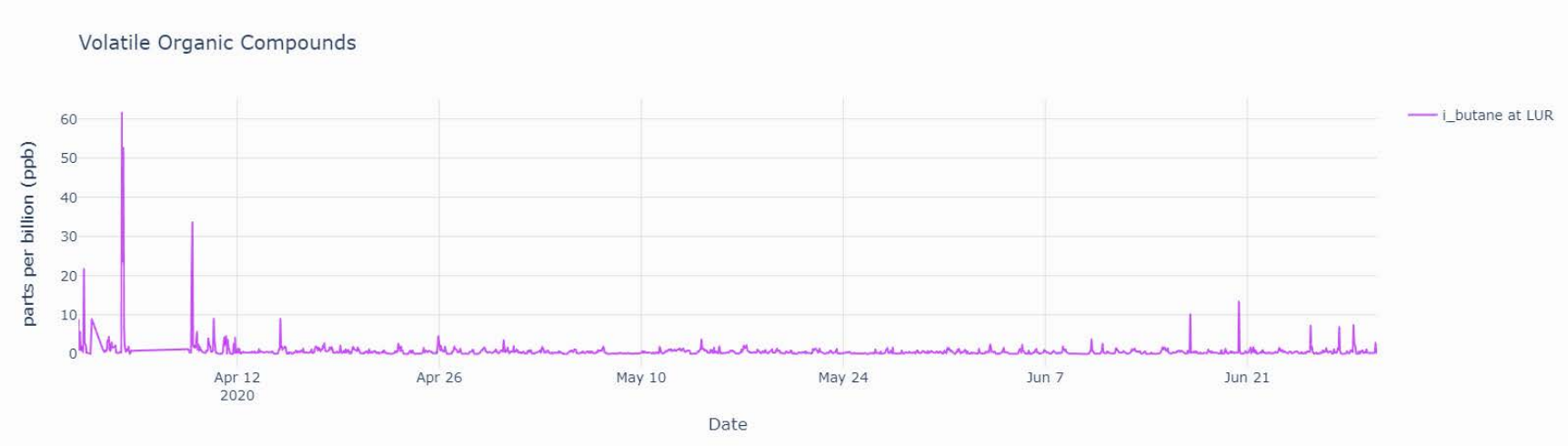

Figure SB12:
LUR i-butane record April 1 – June 30, 2020.

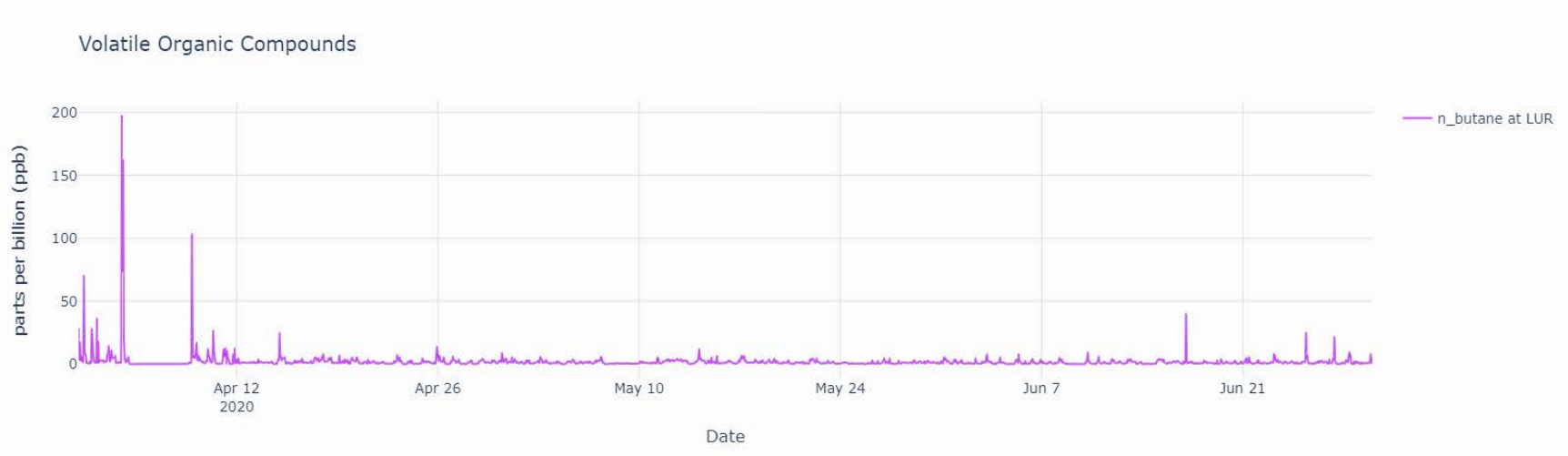

Figure SB13:
LUR n-butane record April 1 – June 30, 2020.

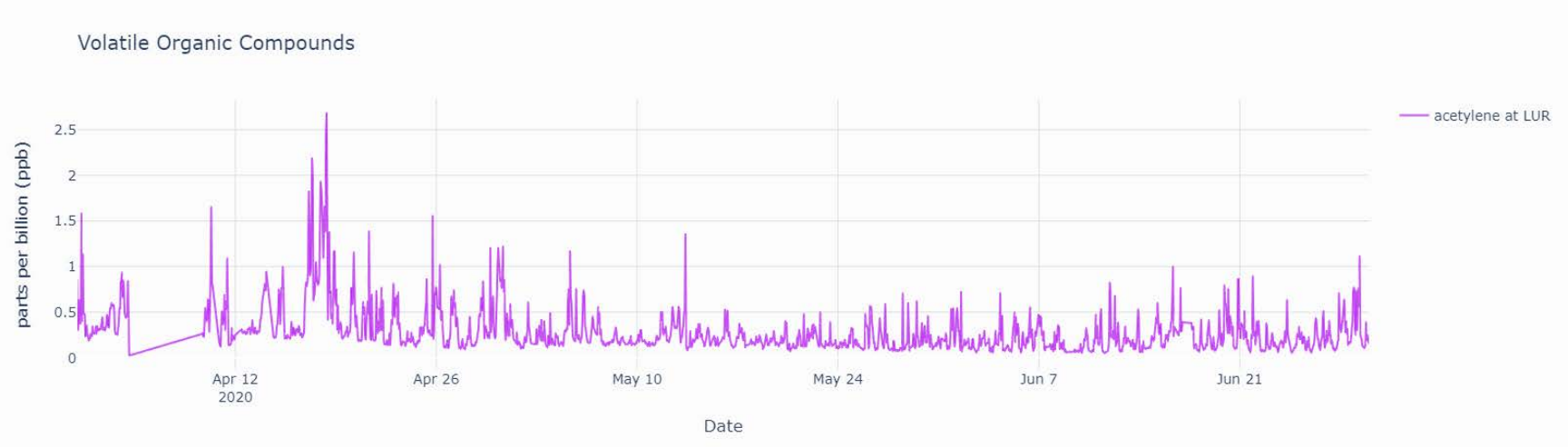

Figure SB14:
LUR acetylene record April 1 – June 30, 2020.

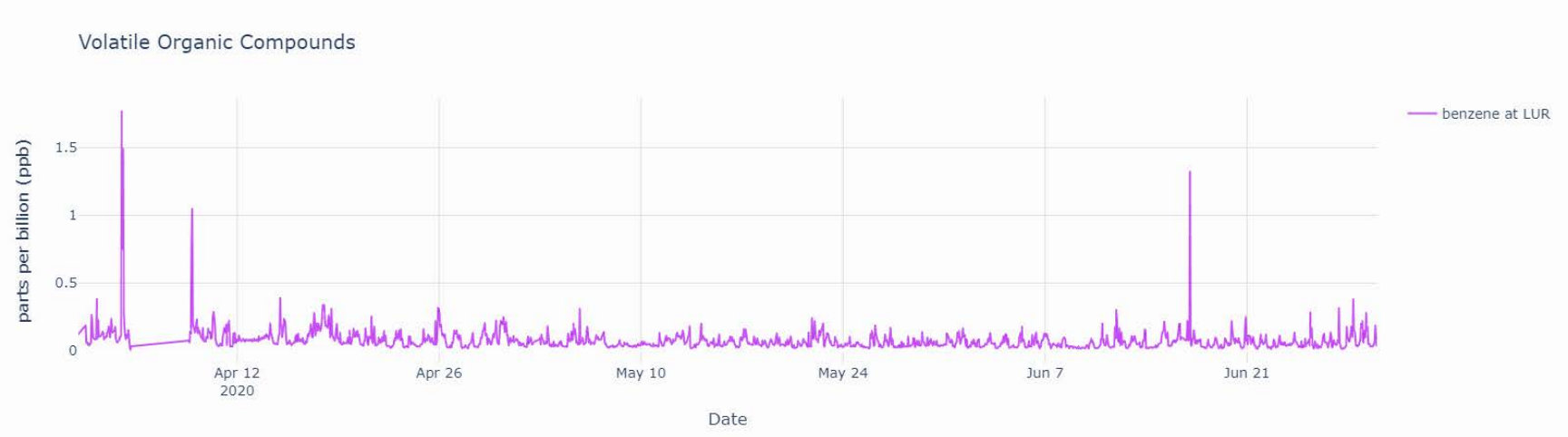

Figure SB15:
LUR benzene record April 1 – June 30, 2020.

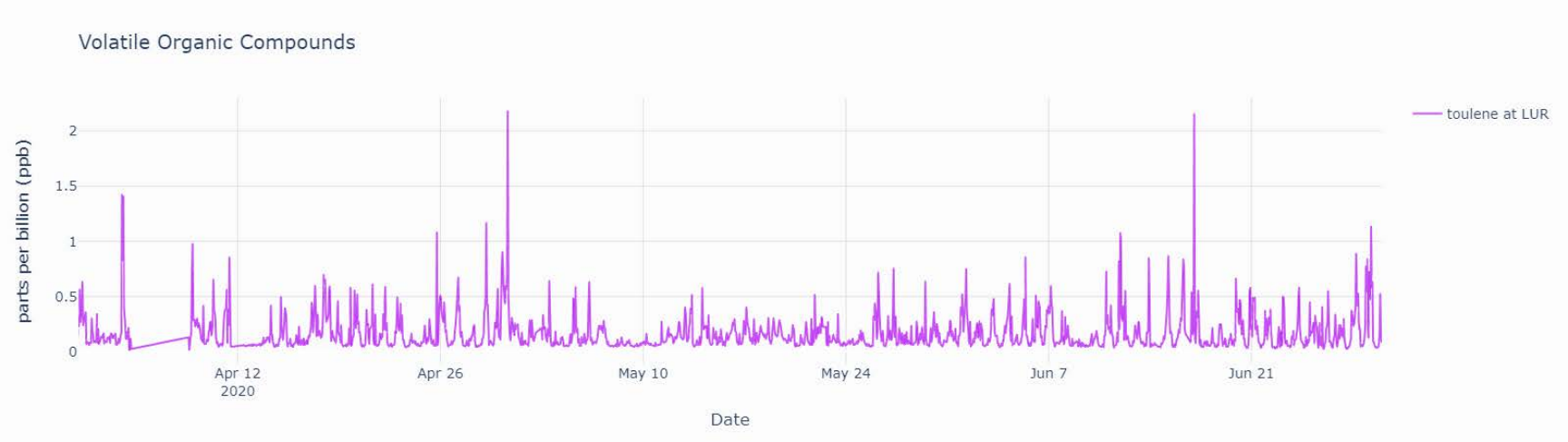

Figure SB16:
LUR toluene record April 1 – June 30, 2020.

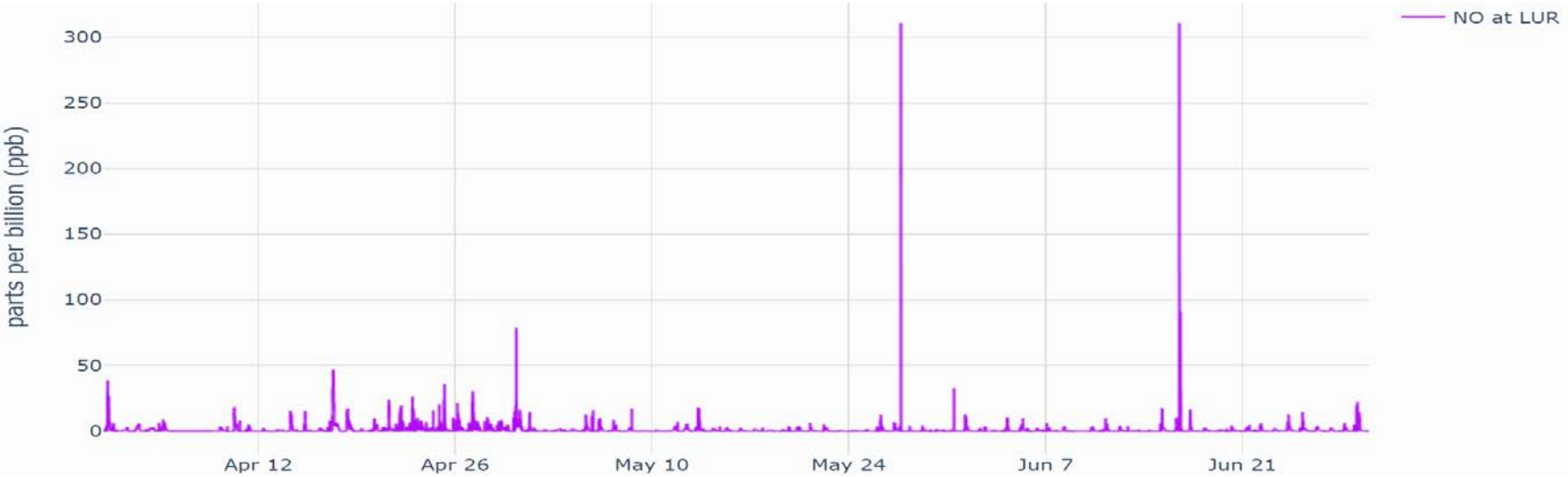

Figure SB17:
LUR nitric oxide record April 1 – June 30, 2020.

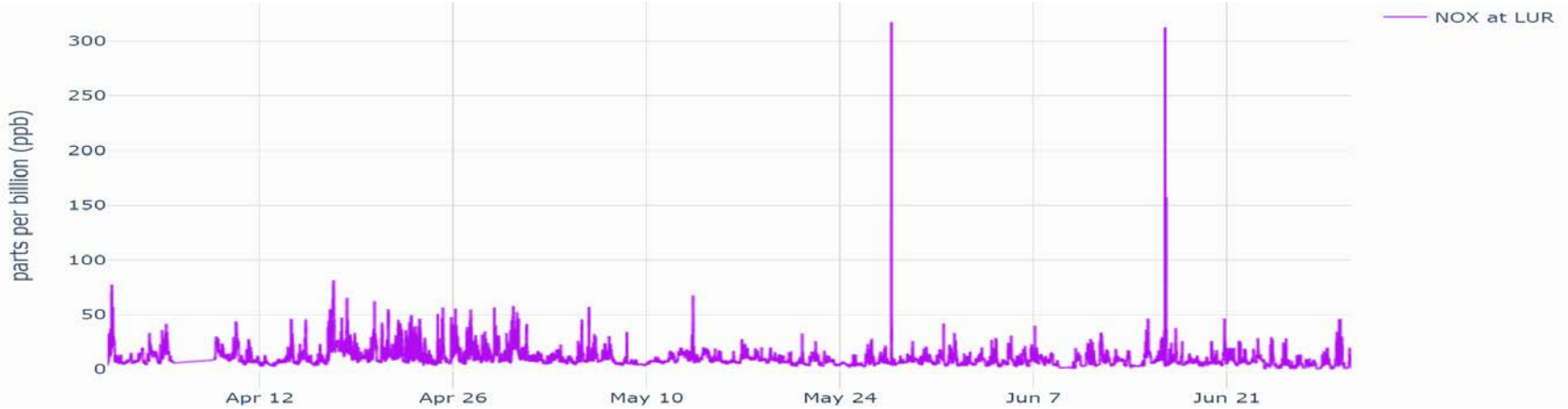

Figure SB18:
LUR nitrogen oxides record April 1 – June 30, 2020.

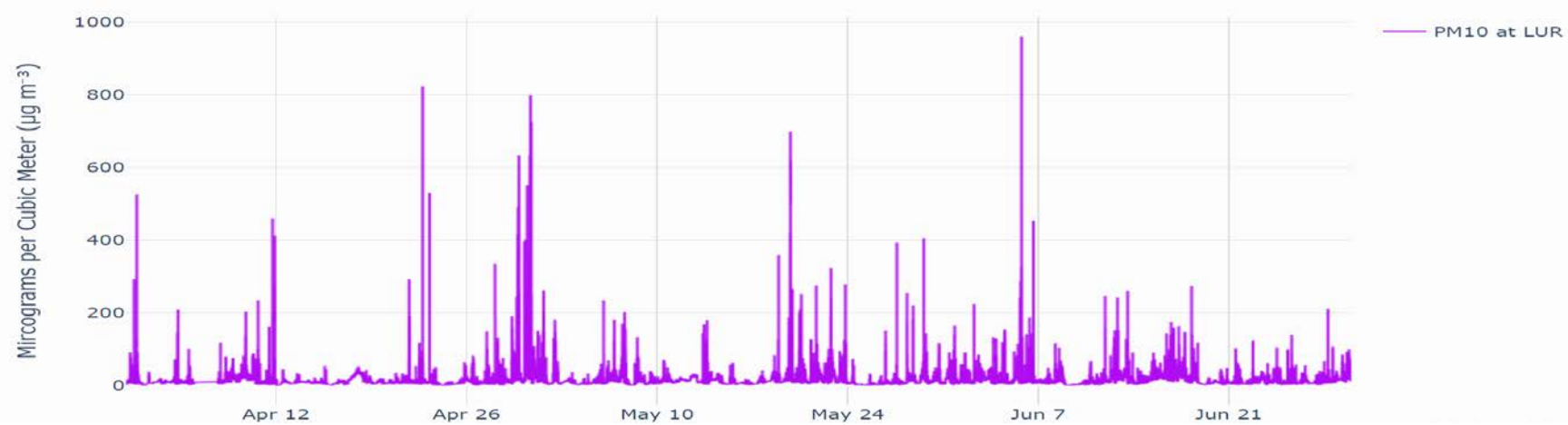

Figure SB19:
LUR coarse particulate matter PM_{10} record for April 1 – June 30, 2020.

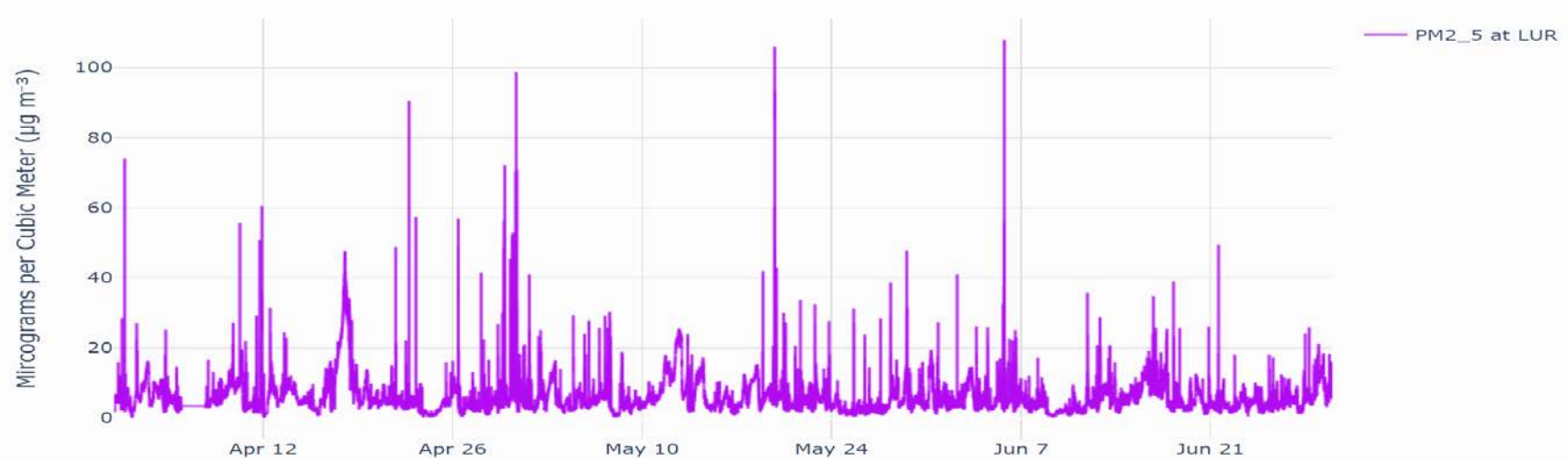

Figure SB20:
LUR fine particulate matter $PM_{2.5}$ record for April 1 – June 30, 2020.

Supplement C

Comparison of Preliminary Data LMA & LUR 2020

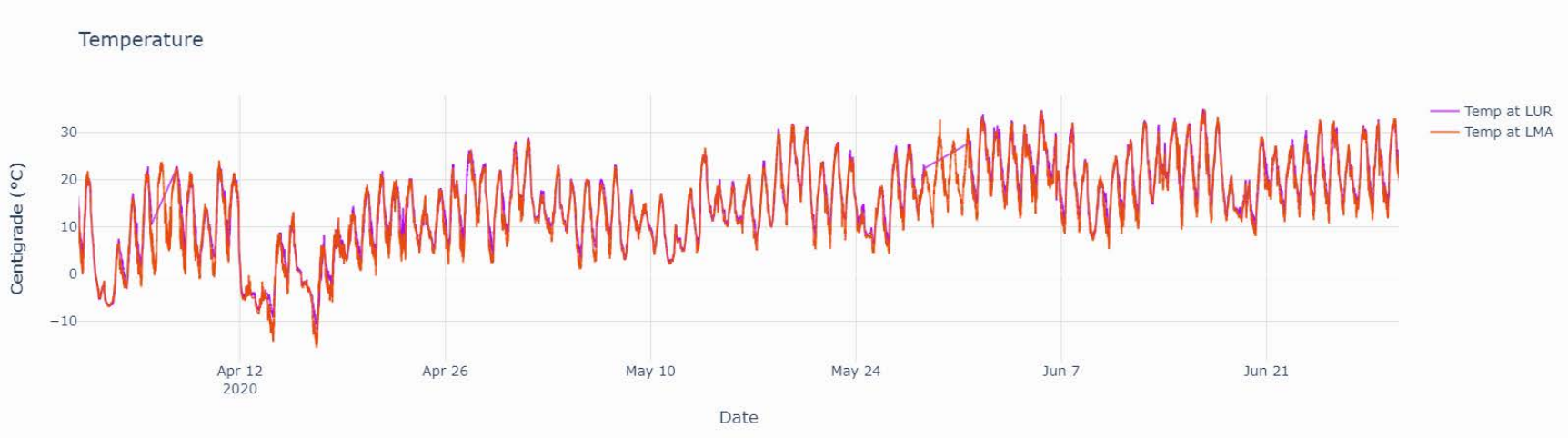

Figure SC1:
LMA & LUR Temperature record April 1 – June 30, 2020.

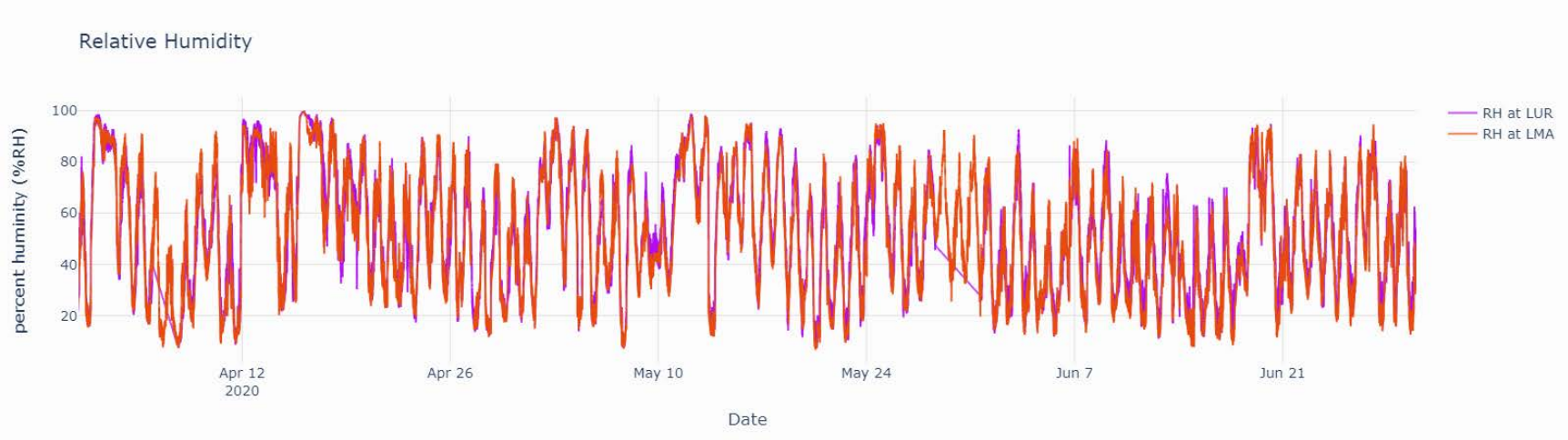

Figure SC2:
LMA & LUR relative humidity record September April 1 – June 30, 2020.

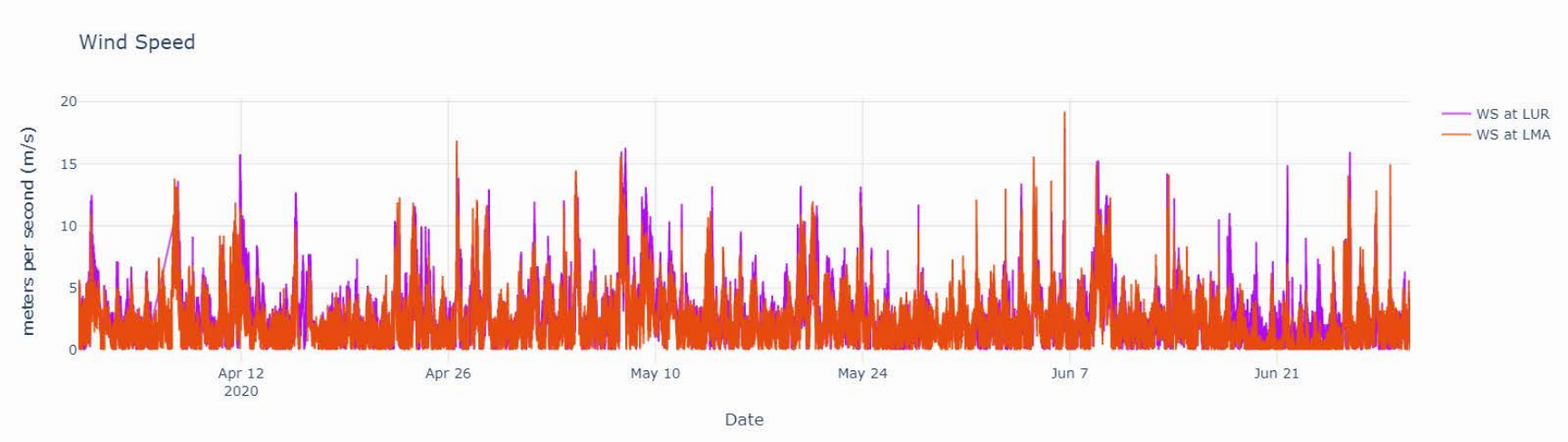

Figure SC3:
LMA & LUR wind speed record April 1 – June 30, 2020.

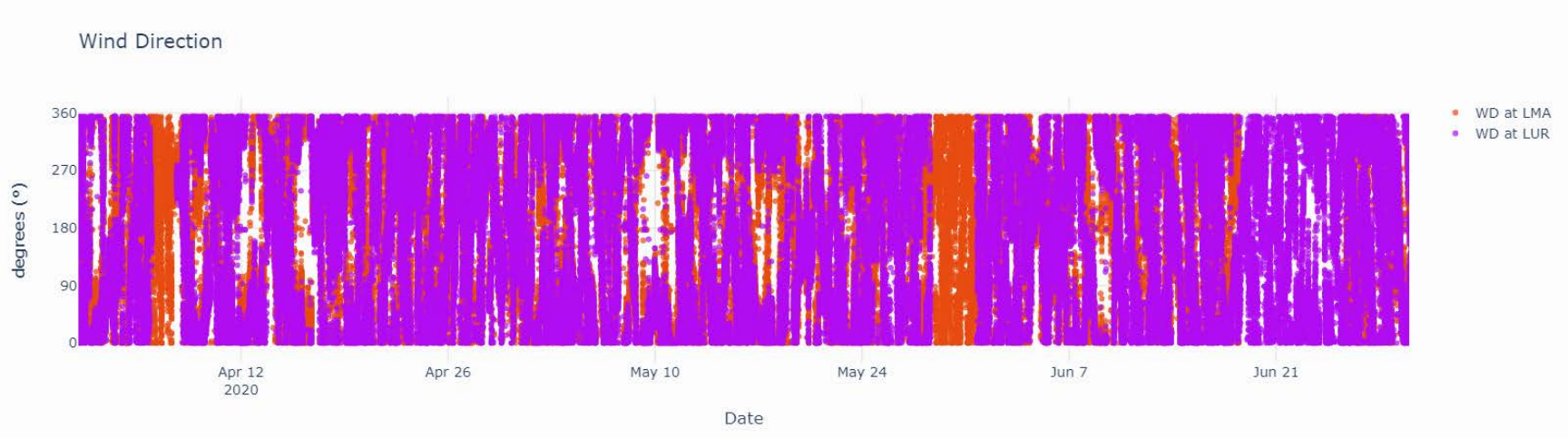

Figure SC4:
LMA & LUR wind direction record April 1 – June 30, 2020.

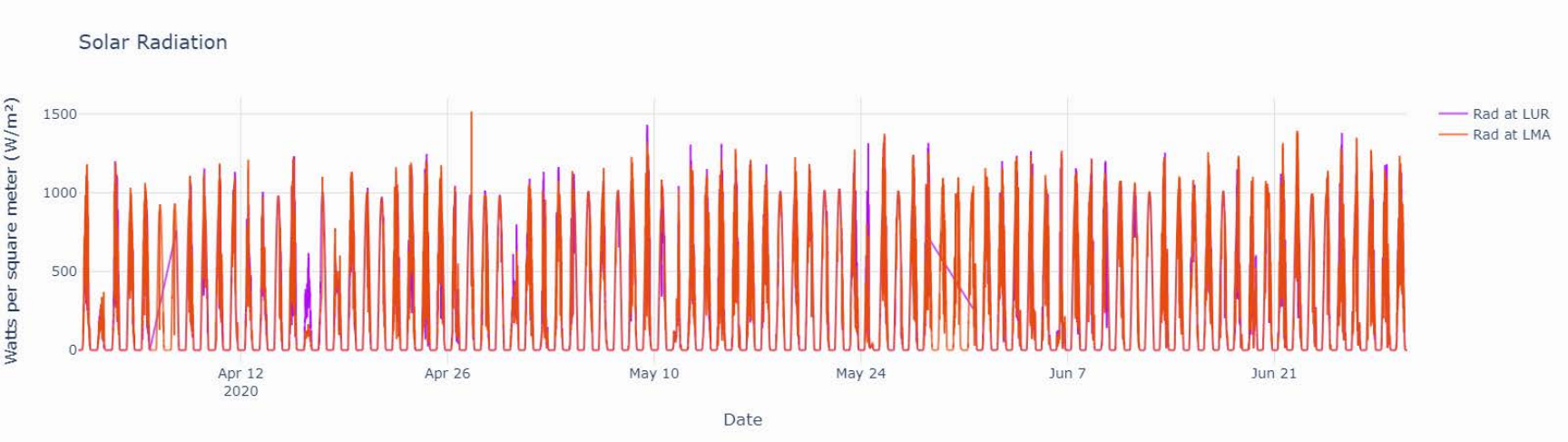

Figure SC5:
LMA & LUR solar radiation record September April 1 – June 30, 2020.

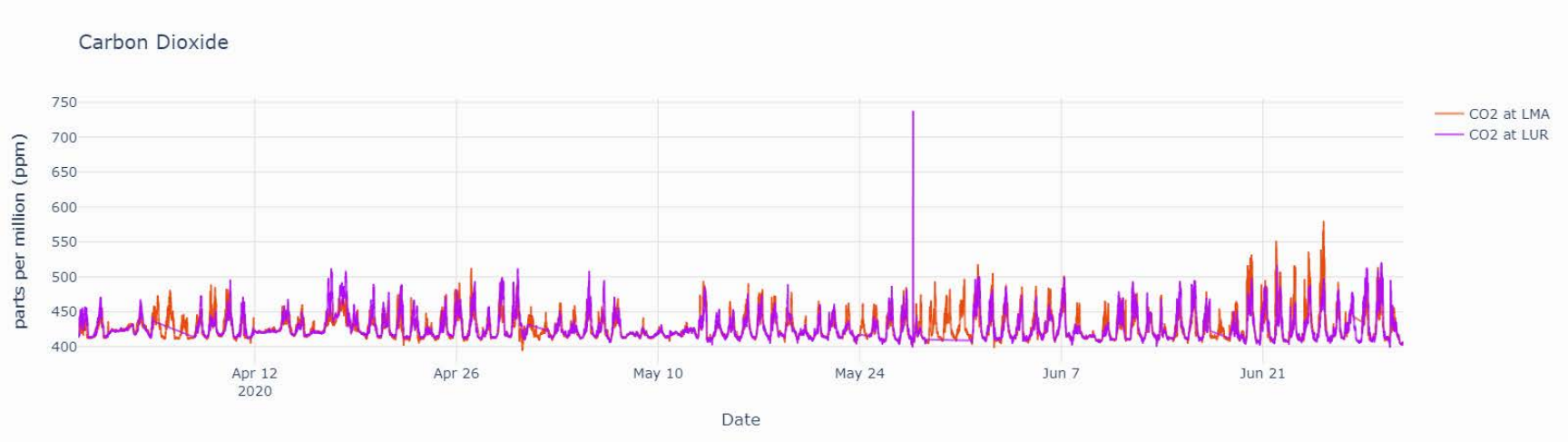

Figure SC6:
LMA & LUR CO_2 record September April 1 – June 30, 2020.

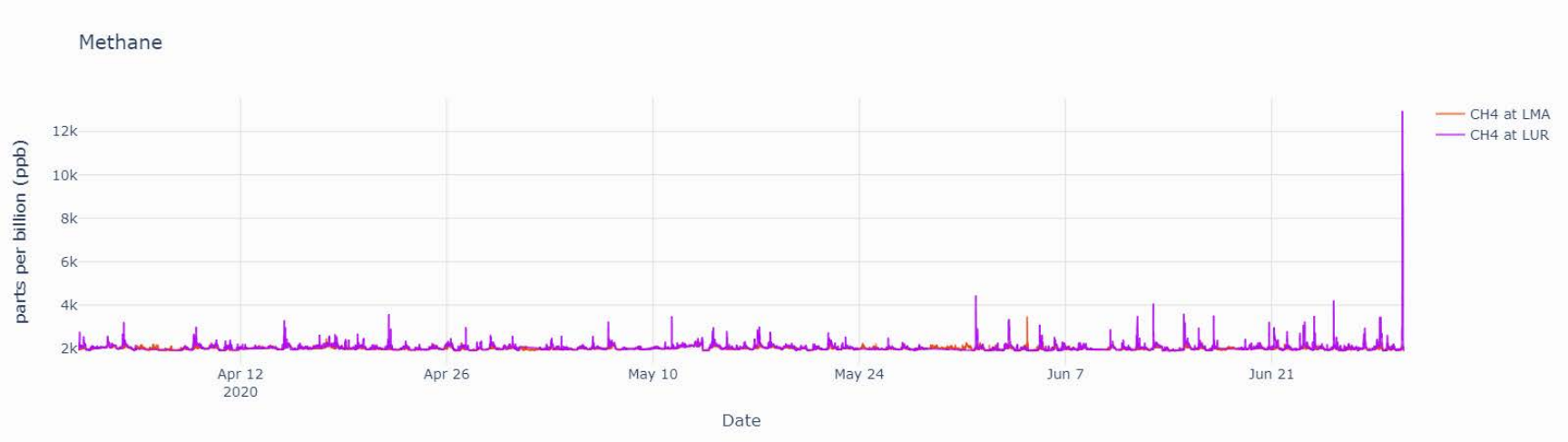

Figure SC7:
LMA & LUR methane record September April 1 – June 30, 2020.

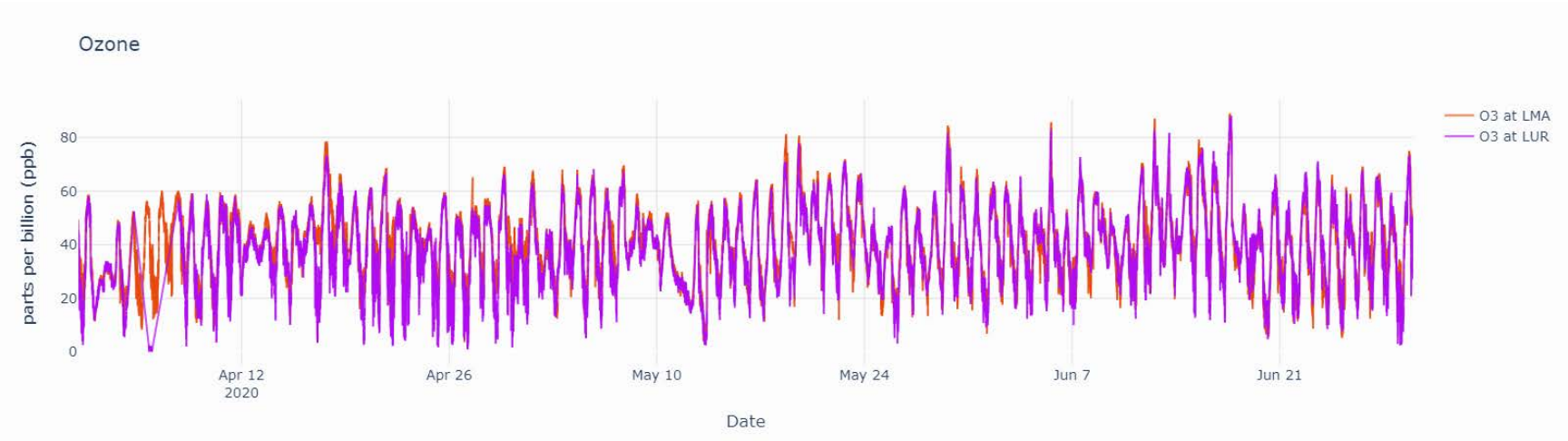

Figure SC8:
LMA & LUR ozone record September April 1 – June 30, 2020.